

TERNARY PHASE EQUILIBRIA IN TRANSITION METAL-
BORON-CARBON-SILICON SYSTEMS

Part II. Ternary Systems
Volume XII. Ti-Zr-B System. Investigation of Pseudo-
Binary Systems ZrB_2 - NbB_2 , ZrB_2 - TaB_2 ,
and HfB_2 - NbB_2 .

T. E. Eckert

~~This document is subject to special export controls, and each transmittal to foreign governments or foreign nationals may be made only with prior approval of Metals and Ceramics Division, Air Force Materials Laboratory, Wright-Patterson Air Force Base, Ohio.~~

**** Export controls have been removed *** for
This document has been approved for
public release and sale; its distribution
is unlimited. U.S.A.F. Systems Command
Letter dated Aug. 22, 1968
MAMC (Capt. Marchiondo)
U 837117*

Report Documentation Page			Form Approved OMB No. 0704-0188		
Public reporting burden for the collection of information is estimated to average 1 hour per response, including the time for reviewing instructions, searching existing data sources, gathering and maintaining the data needed, and completing and reviewing the collection of information. Send comments regarding this burden estimate or any other aspect of this collection of information, including suggestions for reducing this burden, to Washington Headquarters Services, Directorate for Information Operations and Reports, 1215 Jefferson Davis Highway, Suite 1204, Arlington VA 22202-4302. Respondents should be aware that notwithstanding any other provision of law, no person shall be subject to a penalty for failing to comply with a collection of information if it does not display a currently valid OMB control number.					
1. REPORT DATE OCT 1966		2. REPORT TYPE		3. DATES COVERED	
4. TITLE AND SUBTITLE Ternary Phase Equilibrium in Transition Metal-Boron-Carbon-Silicon Systems. Part II Ternary Systems. Vol XII Ti-Zr-B System. Investigation of Pseudo-Binary Systems ZrB₂, -NbB₂, ZrB₂, TaB₂, and HfB₂ -NbB₂				5a. CONTRACT NUMBER	
				5b. GRANT NUMBER	
				5c. PROGRAM ELEMENT NUMBER	
6. AUTHOR(S)				5d. PROJECT NUMBER	
				5e. TASK NUMBER	
				5f. WORK UNIT NUMBER	
7. PERFORMING ORGANIZATION NAME(S) AND ADDRESS(ES) Paul V. Galvin Library, 35 W. 33rd Street, Chicago, IL, 60616				8. PERFORMING ORGANIZATION REPORT NUMBER	
9. SPONSORING/MONITORING AGENCY NAME(S) AND ADDRESS(ES)				10. SPONSOR/MONITOR'S ACRONYM(S)	
				11. SPONSOR/MONITOR'S REPORT NUMBER(S)	
12. DISTRIBUTION/AVAILABILITY STATEMENT Approved for public release; distribution unlimited.					
13. SUPPLEMENTARY NOTES					
14. ABSTRACT					
15. SUBJECT TERMS					
16. SECURITY CLASSIFICATION OF:			17. LIMITATION OF ABSTRACT	18. NUMBER OF PAGES 62	19a. NAME OF RESPONSIBLE PERSON
a. REPORT unclassified	b. ABSTRACT unclassified	c. THIS PAGE unclassified			

FOREWORD

The work described in this report has been carried out at the Materials Research Laboratory, Aerojet-General Corporation, Sacramento, California under USAF Contract No. AF 33(615)-1249. The Contract was initiated under Project No. 7350, Task No. 735001, and was administered under the direction of the Air Force Materials Laboratory, Research and Technology Division, with Captain R. A. Peterson and Lt. P.J. Marchiando acting as Project Engineers, and Dr. E. Rudy, Aerojet-General Corporation as Principal Investigator. Professor Dr. Hans Nowotny, University of Vienna served as consultant to the project.

The project, which includes the experimental and theoretical investigation of selected ternary systems in the system classes Me_1-Me_2-C , $Me-B-C$, Me_1-Me_2-B , $Me-Si-B$, and $Me-Si-C$, was initiated on 1 January 1964.

The author wishes to acknowledge the help received from Dr. E. Rudy, Dr. Y.A. Chang, Dr. C.E. Brukl, D.P. Harmon, and J. Hoffman. Thanks are also due to E. W. Spencer and J. Pomodoro for help preparing samples, and to R. Cristoni for the drawings, and J. Weidner for typing the report.

The excellent book by F. N. Rhines, Phase Diagrams in Metallurgy⁽¹⁾, was extensively consulted in questions regarding nomenclature and interpretation of the equilibria.

The manuscript of this report was released by the author in March, 1966 for publication as an RTD Technical Report.

Other reports issued under USAF Contract AF 33(615)-1249 have included:

Part I. Related Binaries

Volume I.	Mo-C Systems
Volume II.	Ti-C and Zr-C Systems
Volume III.	Mo-B and W-B Systems
Volume IV.	Hf-C System
Volume V.	Ta-C System. Partial Investigation of the Systems V-C and Nb-C
Volume VI.	W-C System, Supplemental Information on the Mo-C System
Volume VII.	Ti-B System
Volume VIII.	Zr-B System
Volume IX.	Hf-B System

Part II. Ternary Systems

Volume I.	Ta-Hf-C System
Volume II.	Ti-Ta-C System
Volume III.	Zr-Ta-C System
Volume IV.	Ti-Zr-C, Ti-Hf-C and Zr-Hf-C System.
Volume V.	Ti-Hf-B System

FOREWORD (Cont'd)

Volume VI.	Zr-Hf-B System
Volume VII.	Ti-Si-C, Nb-Si-C, and W-Si-C Systems
Volume VIII.	Ta-W-C System
Volume IX.	Zr-W-B System, Pseudobinary System TaB ₂ -HfB ₂
Volume X.	Zr-Si-C, Hf-Si-C, Zr-Si-B, and Hf-Si-B Systems
Volume XI.	Hf-Mo-B and Hf-W-B Systems

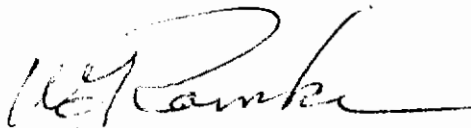
Part III. Special Experimental Techniques

Volume I.	High Temperature Differential Thermal Analysis
-----------	---

Part IV. Thermochemical Calculations

Volume I.	Thermodynamic Properties of Group IV, V, and VI Transition Metal Carbides
Volume II.	Thermodynamic Interpretation of Ternary Phase Diagrams.
Volume III.	Computational Approach to the Calculation of Ternary Phase Diagrams

This technical report has been reviewed and is approved.



W. G. RAMKE
Chief, Ceramics and Graphite Branch
Metals and Ceramics Division
Air Force Materials Laboratory

ABSTRACT

The ternary system titanium-zirconium-boron was investigated from 1000°C to 3245°C, the melting temperature of zirconium diboride. The equilibria which exist have been determined except for the boron-rich equilibria which have been estimated. The following notable features were found: minimum melting occurs in the titanium rich corner of the ternary; a four-phase reaction involving β -metal phase, monoboride, diboride, and liquid occurs at a temperature slightly higher than the minimum melting; zirconium exchanges with titanium in titanium monoboride to about 9 At.% zirconium; and the metal diborides form a continuous series of solid solutions. No ternary compounds were found. The techniques used in the investigation were X-ray analysis, melting point determination, and metallographic examination. Lattice parameter plots of the pseudo-binary systems ZrB_2 - NbB_2 , ZrB_2 - TaB_2 , and HfB_2 - NbB_2 indicate that in each of these systems the diborides form a continuous series of solid solutions. Melting point temperatures for these systems have been determined.

Contrails

TABLE OF CONTENTS

	PAGE
I. INTRODUCTION AND SUMMARY	1
A. Introduction	1
B. Summary	1
1. Titanium-Zirconium-Boron	1
2. Pseudo-Binaries ZrB_2 - NbB_2 , ZrB_2 - NbB_2 , and HfB_2 - NbB_2	5
II. LITERATURE REVIEW	6
A. Boundary Systems	6
1. Titanium-Zirconium Binary	6
2. Metal-Boron Binaries	7
B. Titanium-Zirconium-Boron Ternary System	7
C. The Pseudo-Binaries ZrB_2 - NbB_2 , ZrB_2 - TaB_2 , and HfB_2 - NbB_2	8
III. EXPERIMENTAL PROGRAM	9
A. Experimental Procedures	9
1. Starting Materials	9
2. Alloy Preparation and Heat Treatment	10
3. Melting Points	10
4. Metallography	11
5. X-Ray Analysis	12
IV. RESULTS	12
A. Low-Temperature Equilibria--The Solid State Section at 1400°C	12
B. High-Temperature Equilibria	22
C. Investigation of the Melting Temperatures of the Solid Solutions $(Zr, Nb)B_2$, $(Zr, Ta)B_2$, and $(Hf, Nb)B_2$	39

TABLE OF CONTENTS (Cont'd)

	PAGE
V. DISCUSSION	46
References	47

LIST OF ILLUSTRATIONS

FIGURE		PAGE
1	Titanium-Zirconium-Boron Phase Diagram	3
2	Scheil-Schultz Diagram for the System Titanium-Zirconium-Boron	4
3	Ti-Zr-B: Isopleth Across 20 Atomic Percent Boron	5
4	Phase Diagram Titanium-Zirconium	6
5	Phase Diagram Titanium-Boron	7
6	Phase Diagram Zirconium-Boron	8
7	Composition of Alloys Studied Metallographically	11
8	Composition of Alloys Investigated for the Solid State Section at 1400°C	13
9	Isothermal Section at 1400°C	13
10	Primary Monoboride and Monoboride-Metal Eutectic. Ti-Zr-B: 60-10-30.	14
11	Micrograph of Ti-Zr-B (79-13-8) Alloy Near the Metal-Metal Monoboride Eutectic Trough.	15
12	Micrograph of an Arc-Melted Ti-Zr-B (20-50-30) Alloy	15
13	Micrograph of an Arc-Melted, Ti-Zr-B (10-60-30) Alloy.	16
14	Micrograph of Ti-Zr-B (21-68-11) Alloy	16
15	Micrograph of Ti-Zr-B (40-30-30) Alloy	17
16	Micrograph of Ti-Zr-B (25-25-50), Alloy.	17
17	Micrograph of an Arc-Melted Ti-Zr-B (22-25-53) Alloy	18
18	Micrograph of Ti-Zr-B (40-10-50) Alloy	19
19	Lattice Parameters of Ternary Diboride Alloys Equilibrated at 1400°C	20
20	Micrograph of Ti-Zr-B (28-5-67) Alloy.	21
21	Melting Points and Position of Metal-Rich Eutectic Trough	22
22	Isothermal Section at 1445°C	24

LIST OF ILLUSTRATIONS (Cont'd)

FIGURE		PAGE
23	Isotherm at 1450°C	24
24	Plot of Liquidus Projections	27
25	Observed Melting Temperatures of Ternary Diboride Alloys	28
26	Isothermal Section at 1400°C	29
27	Isothermal Section at 1445°C	30
28	Isothermal Section at 1445°C + ΔT_1	30
29	Isothermal Section at 1450°C	31
30	Isothermal Section at 1450°C + ΔT_2	31
31	Isothermal Section at 1580°C	32
32	Isothermal Section at 1620°C	32
33	Isothermal Section at 1660°C	33
34	Isothermal Section at 1725°C	33
35	Isothermal Section at 2000°C	34
36	Isothermal Section at 2020°C	35
37	Isothermal Section at 2040°C	36
38	Isothermal Section at 2100°C	37
39	Isothermal Section at 2300°C	38
40	Isothermal Section at 3225°C	39
41	Lattice Parameters of Pseudo-Binary ZrB_2-NbB_2	40
42	Melting Point Temperatures of Pseudo-Binary ZrB_2-NbB_2	40
43	Lattice Parameters of Pseudo-Binary ZrB_2-TaB_2	41
44	Melting Point Temperatures of Pseudo-Binary ZrB_2-TaB_2	41
45	Lattice Parameters of Pseudo-Binary HfB_2-NbB_2	42
46	Melting Point Temperatures of Pseudo-Binary HfB_2-NbB_2	42
47	Metallography of ZrB_2-NbB_2 : 60-40 Mole %	43

LIST OF ILLUSTRATIONS (Cont'd)

FIGURE		PAGE
48	Metallography of ZrB_2 - TaB_2 : 10-90 Mole %	44
49	Metallography of HfB_2 - NbB_2 : 20-80 Mole %	45

LIST OF TABLES

TABLE		PAGE
1	Composition of the Phases Participating in the Four-Phase Reaction at 1450°C	23
2	Results of Melting Point Investigations	25

I. INTRODUCTION AND SUMMARY

A. INTRODUCTION

The purpose of this investigation was to determine the nature of the equilibria which exist in the ternary system titanium-zirconium-boron from 1000°C to the melting point of zirconium diboride. This investigation is part of a larger program initiated by the United States Air Force in this laboratory for the investigation of phase equilibria in selected ternary systems containing transition metals, boron, carbon, and silicon.

This system is of interest because of the oxidation resistance of the diborides and because of their refractoriness. The poor thermal shock characteristics of the diborides lead to the consideration of the diborides in a composite structure, such as metal plus the metal diboride. This is to overcome the thermal shock problems while taking advantage of the oxidation resistance and the refractoriness of the diborides. To this end, the high temperature equilibria of the titanium and zirconium diborides with their elemental constituents have been investigated.

B. SUMMARY

1. Titanium-Zirconium-Boron

a. The Hexagonal (C-32) Diboride Phase (8)

Titanium diboride ($a = 3.025 \text{ \AA}$, $c = 3.226 \text{ \AA}$) and zirconium diboride ($a = 3.167 \text{ \AA}$, $c = 3.530 \text{ \AA}$) form a continuous series of solid solutions. The lattice parameters very nearly follow Vegard's law. The melting points of the diboride alloys were investigated (Figure 25).

b. The Orthorhombic (B-27) Monoboride Phase (γ)

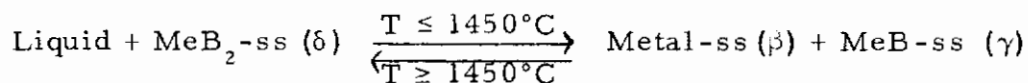
The maximum exchange of zirconium for titanium in titanium monoboride is approximately 9 At.%. The lattice parameters of titanium diboride are; $a = 6.14 \text{ \AA}$, $b = 3.06 \text{ \AA}$, $c = 4.57 \text{ \AA}$.

c. The High Temperature B.C.C. (A-2) (β) Metal Phase

The high temperature β phase of the metal solid solution was partially retained by rapid cooling from 1400°C in several metal-rich ternary samples. A lattice parameter of the sample Ti-Zr-B: 45-45-10 measured 3.46 \AA . Solubility of boron in the individual metals is slight and is assumed to be slight in the ternary.

d. Class II Four-Phase Equilibria at 1450°C

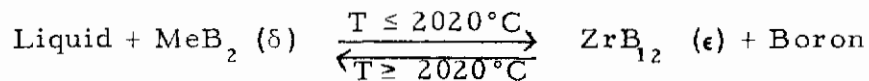
The four-phase reaction at 1450°C is represented by the reaction equation



The isotherm at 1450°C shows the four-phase reaction. Another four-phase reaction occurs in the metal-rich region at lower temperatures, but this reaction occurs well below 1000°C and was beyond the limits of this investigation.

(1) Class II Four-Phase Equilibrium at 2020°C

Another four-phase reaction must occur in this system somewhere in the temperature range 2000°C to 2080°C . This reaction was not investigated. It is indicated in the space model (Figure 1) at 2020°C . The equation for the reaction is presumed to be



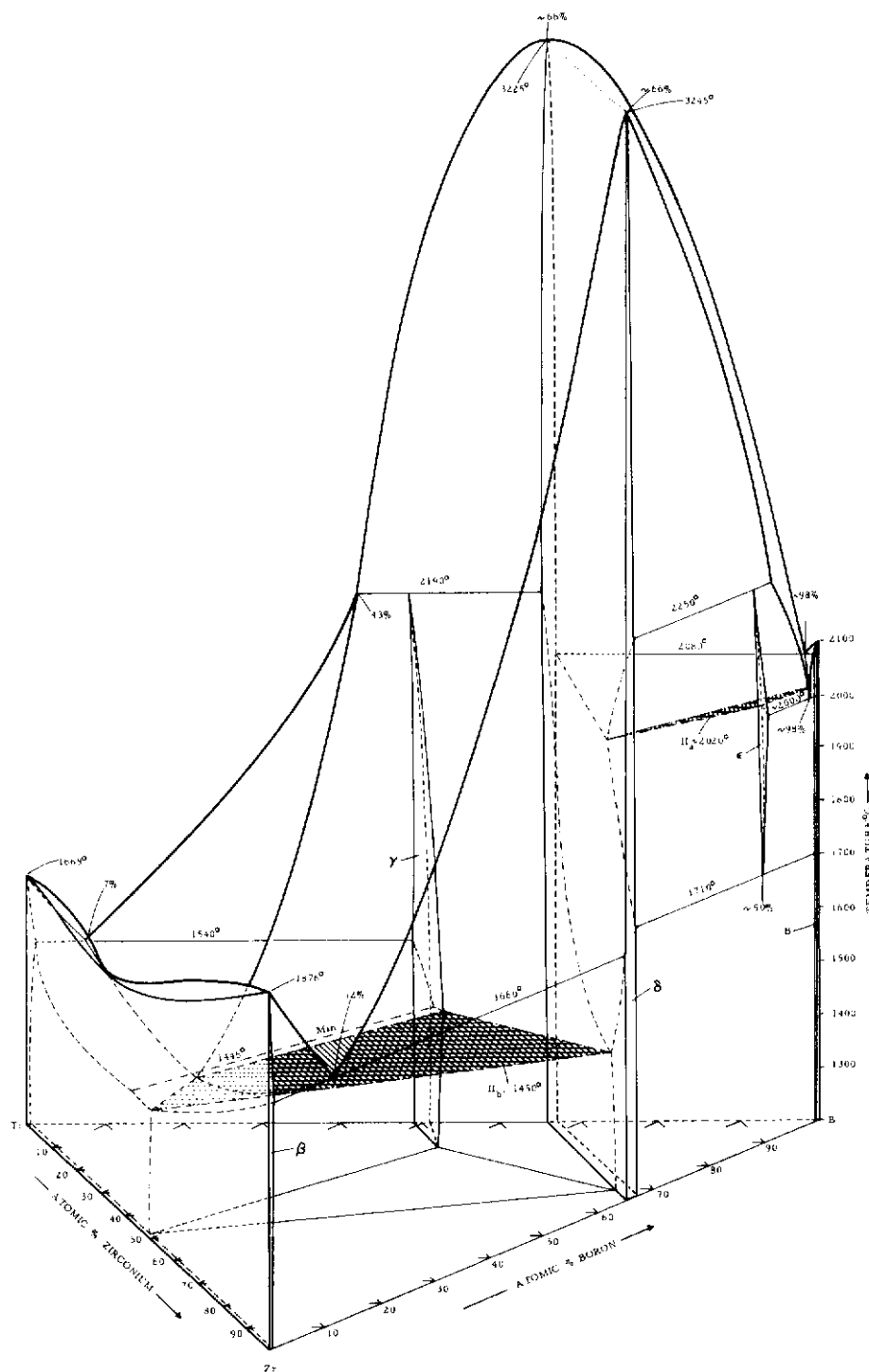


Figure 1. Titanium-Zirconium-Boron Phase Diagram

e. Limiting Tie-Line

Because of the initial melting in the ternary at the minimum melting temperature of the eutectic trough, a minimum tie-line exists. With decreasing temperature, the two three-phase regions which result from the presence of the liquid in the ternary, merge into a limiting tie-line. This is shown in Figure 22.

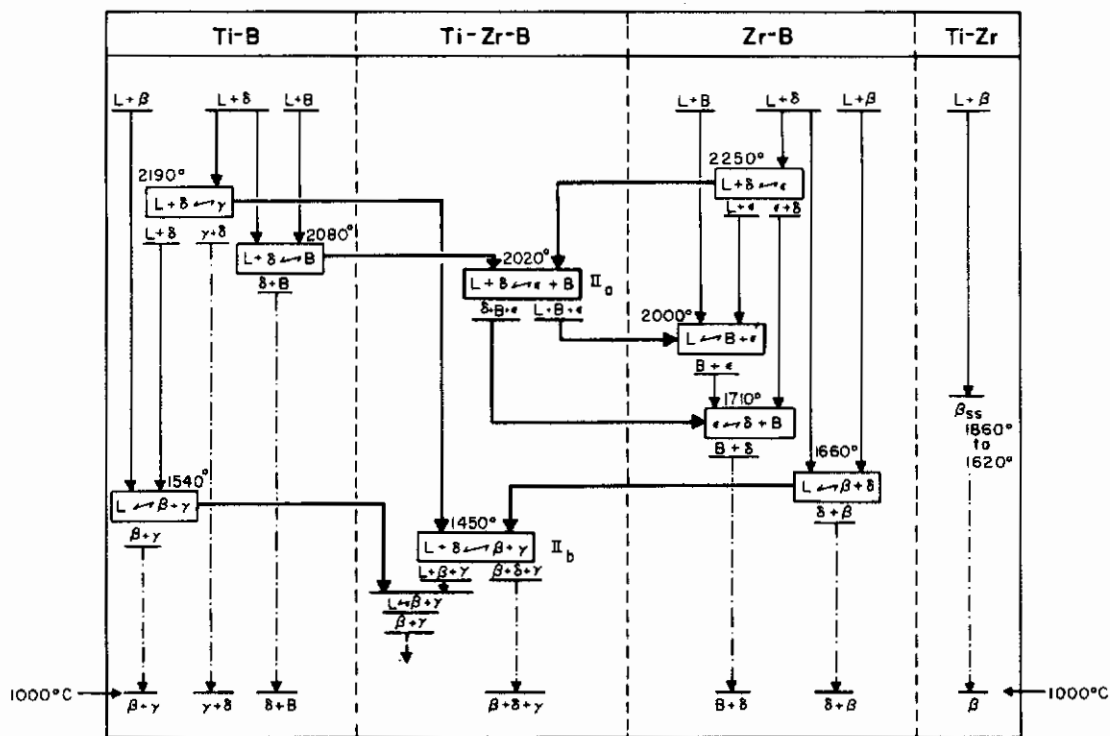


Figure 2. Scheil-Schultz Diagram for the System Titanium-Zirconium-Boron.

f. Space Model for the System Titanium-Zirconium-Boron

The space model for this system has been constructed as is shown in Figure 1. In order to facilitate use of the diagram, a Scheil-Schultz diagram and an isopleth at 20 At. % boron have also been included for this system in Figures 2 and 3.

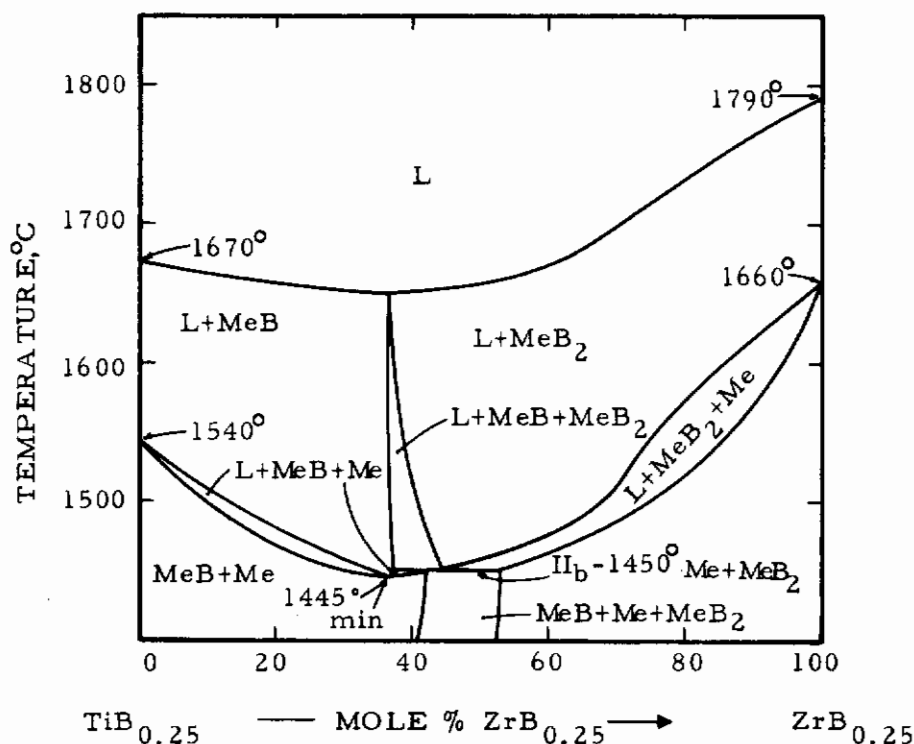


Figure 3. Ti-Zr-B: Isopleth Across 20 Atomic Percent Boron

2. Pseudo-Binaries ZrB₂-NbB₂, ZrB₂-NbB₂, and HfB₂-NbB₂

The results of this investigation confirm the formation of a continuous series of solid solutions in (Zr,Nb)B₂, (Zr,Ta)B₂, and (Hf,Nb)B₂. Lattice parameter plots and melting point plots are given (Figures 41-46).

II. LITERATURE REVIEW

A. BOUNDARY SYSTEMS

1. Titanium-Zirconium Binary

The titanium-zirconium binary system was investigated by Hayes, Roberson, and Paasche⁽²⁾, whose work was, in large part, the basis for the equilibrium diagram given by Hansen⁽³⁾ and shown in Figure 4.

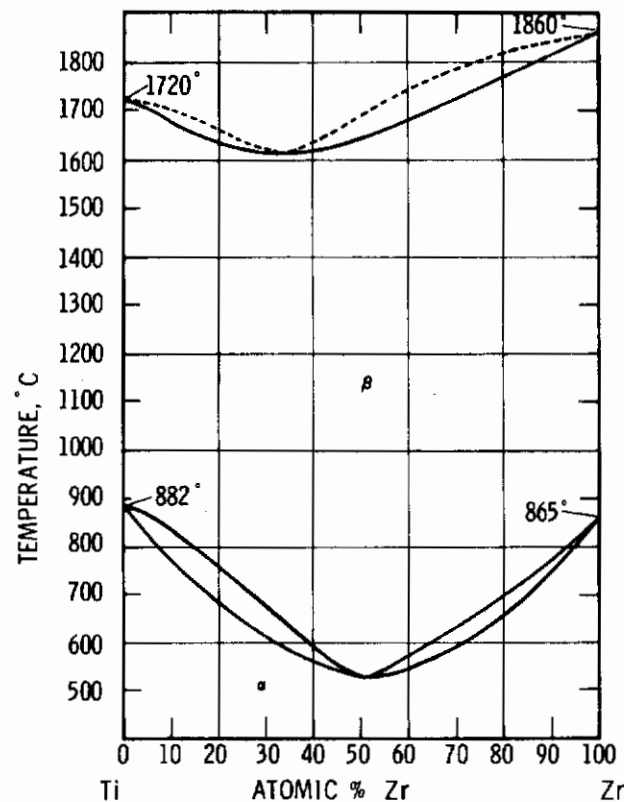


Figure 4. Phase Diagram Titanium-Zirconium.

(Hansen, Constitution of Binary Alloys, 1958)

As shown in the diagram, both the α and β phases of the metal are completely miscible. The α - β transformation and melting curves both have a minimum in this system.

2. Metal-Boron Binaries

Both the titanium-boron and the zirconium-boron binaries have recently been investigated in this laboratory by E. Rudy and St. Windisch and are described in previously issued documentary reports^(4, 5). The phase diagrams for these systems are shown in Figures 5 and 6.

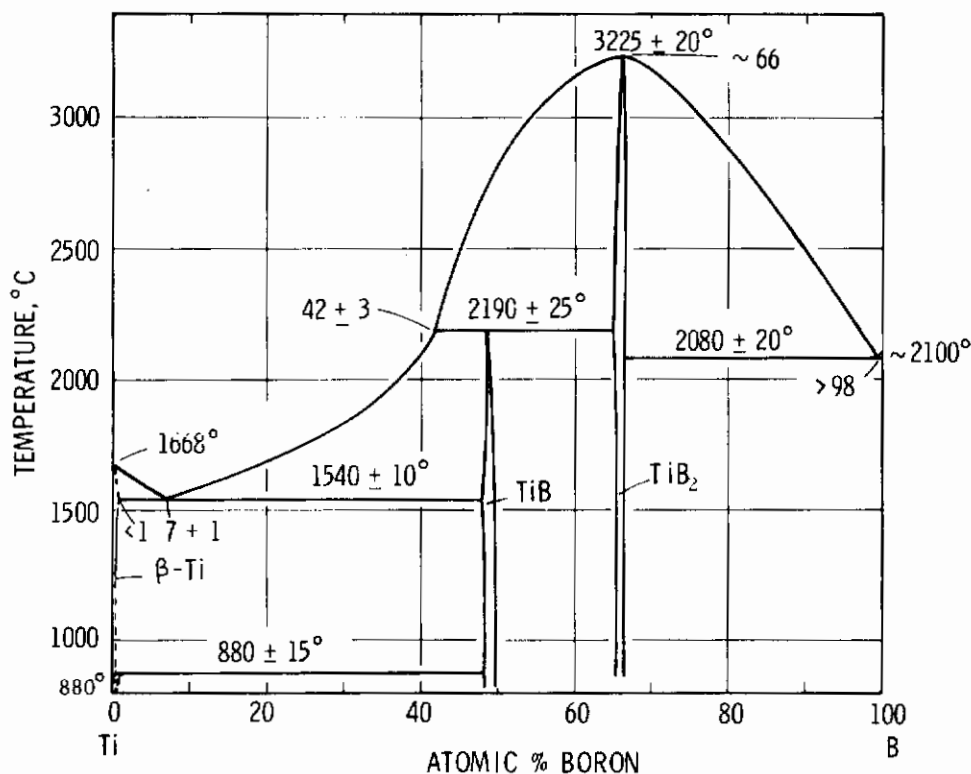


Figure 5. Phase Diagram Titanium-Boron.

B. TITANIUM-ZIRCONIUM-BORON TERNARY SYSTEM

Titanium diboride and zirconium diboride form a continuous series of solid solutions^(6, 7, 8, 9, 10). The lattice parameters vary nearly linearly between those of the binary compounds^(7, 9, 10). Some work has been done on establishment of the melting points⁽⁹⁾. Microhardness, resistivity, and corrosion properties of the ternary diboride alloys have also been

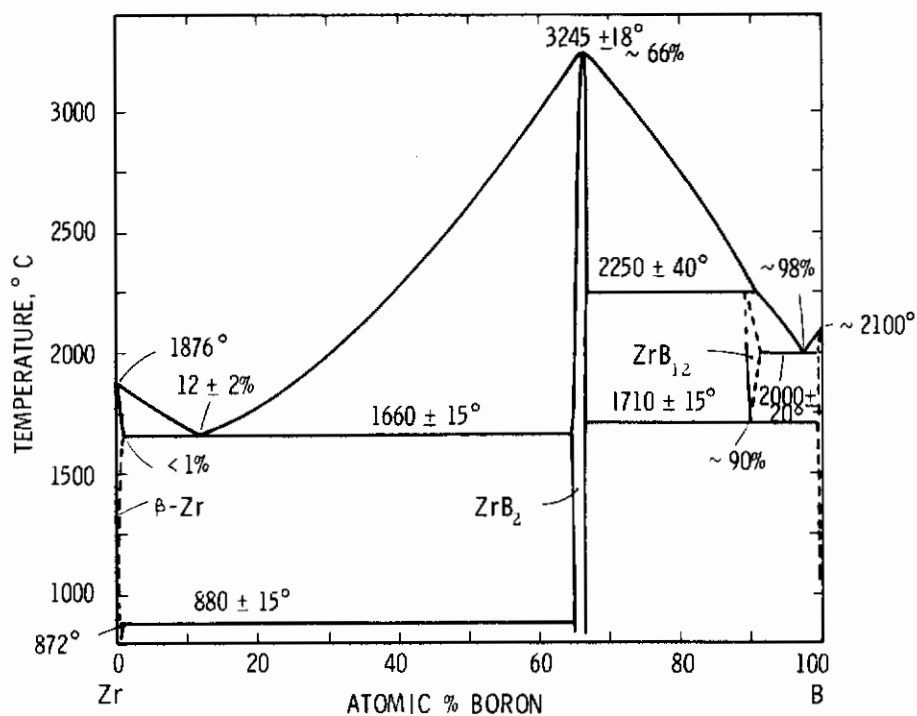


Figure 6. Phase Diagram Zirconium-Boron

investigated⁽¹⁰⁾. Other than the diboride solid solution, no work was found in the literature on the ternary system.

C. THE PSEUDO-BINARIES ZrB₂-NbB₂, ZrB₂-TaB₂, and HfB₂-NbB₂

The formation of continuous series of solid solutions in the pseudo-binaries ZrB₂-NbB₂ and ZrB₂-TaB₂ has been experimentally established by B. Post, F.W. Glaser, and D. Moskowitz⁽⁸⁾, who concluded from considerations of atom sizes that HfB₂-NbB₂ also forms a continuous series of solid solutions.

III. EXPERIMENTAL PROGRAM

A. EXPERIMENTAL PROCEDURES

1. Starting Materials

All alloys investigated were made from combinations of diboride powders prepared here in our laboratory and from elemental powders. Titanium powder was obtained from Var-Lac-Oid Chemical Company, New York, and had the following impurities (in weight percent); C-0.13, H-0.15, N-0.005, Fe-0.05, and Cl-0.12. The powder was sized to less than 65 micrometers.

Zirconium metal powder of particle size less than 74 micrometers was purchased from Wah Chang Company, Albany, Oregon, and had the following impurities (in ppm): Al-55, B-0.2, C-90, Cb-<100, Cd-<0.2, Co-<5, Cr-97, Cu-<25, Fe-470, H-700, Hf-75, Mg-<10, Mn-<10, N-220, Ni-20, O-1350, Pb-<5, Sn-175, Ta-<200, Ti-25, V-5, and W-<25.

Boron powder sized between 174 and 44 micrometers was purchased from United Mineral and Chemical Corp., New York. The boron powder had the following impurities (in weight percent): Fe-0.6, Si-0.1, C-0.1, and other-0.1.

The preparations of the titanium diboride and zirconium diboride powders are described in previous reports^(4, 5). Carbon analysis of the zirconium diboride powder showed it to contain 0.016 percent carbon by weight.

The samples of the ZrB_2 - NbB_2 , ZrB_2 - TaB_2 , and HfB_2 - NbB_2 pseudo-binary systems were made from diboride powders prepared here in our laboratory in the same manner as the titanium and zirconium diborides mentioned above. The hafnium diboride

contained 67.6 At.% boron (and 0.011 Wt.% carbon); the niobium diboride contained 68.8 At.% boron (and 0.088 Wt.% carbon); the zirconium diboride contained 65.2 At.% boron (and 1.358 Wt.% carbon); and the tantalum diboride contained 72 At.% boron (and 0.053 Wt.% carbon).

2. Alloy Preparation and Heat Treatment

All alloys investigated were hot-pressed; the carbide surface layer was ground off to reduce the possibility of contamination. Most samples were then melted in the Pirani furnace as described in a previous report⁽¹¹⁾; additionally, a few sample compositions for the solid-state section were duplicated without melting in the Pirani furnace as a check on possible composition shifts. Samples for the solid state investigation were heat-treated for 100 hours at 1400°C under vacuum (2×10^{-6} Torr). Many of the samples were halved before heat-treating with one half being arc-melted. Both halves were heat-treated. The samples were rapidly cooled by introducing helium into the furnace immediately after shutting off the power. In spite of the long heat-treatment, samples in the ternary system near (Ti,Zr)B did not attain equilibrium due to the slowness of the diffusion limited peritectic reaction.

3. Melting Points

Melting point determination techniques and temperature corrections associated with the technique have been previously described⁽¹¹⁾. All samples were melted in a helium atmosphere of 20 psi after a short degassing treatment at 1200 - 1500°C. Temperature measurements were made with a disappearing filament-type pyrometer calibrated against a National Bureau of Standards certified standard lamp. Approximately 40 samples in the ternary system were melted (see Table 2).

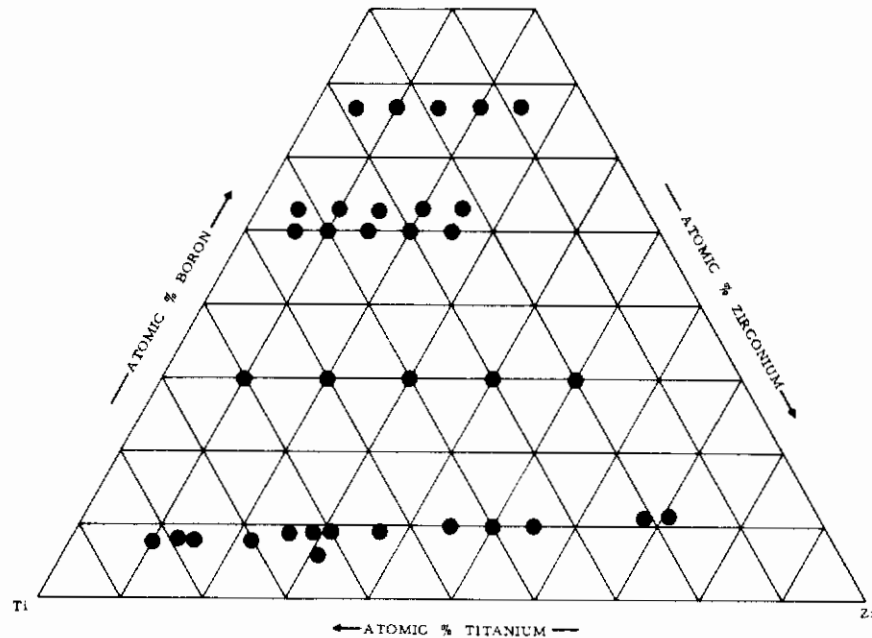


Figure 7. Composition of Alloys Studied Metallographically.

4. Metallography

Approximately 50 samples of 34 various compositions (Figure 7) were studied metallographically, although some were the same alloys with different heat treatments. The samples were mounted in a diallyl-phthalate-lucite-copper

powder such as to provide a conductive path to the sample for electroetching. After mounting, the samples were coarse ground on silicon carbide papers with grit sizes between 120 and 600. Final polishing was done with a slurry of 0.3 micrometer alumina and a 5% solution of chromic acid on nylon cloth. The samples were electroetched in a 0.5% oxalic acid solution.

5. X-Ray Analysis

Debye-Scherrer powder diffraction patterns using CuK_α radiation were made of all samples after their heat-treatment. The structures of all binary phases were known so that indexing of the patterns was no problem. Many of the films were not usable for determining lattice parameters due to non-equilibrium conditions in the samples. The α - β transformation in the metal phase tended to render some of the films useless for lattice parameter measurement since the diffraction lines were quite broad and very diffuse. The use of cover films helped reduce the amount of film darkening due to self-fluorescence caused by the titanium.

IV. RESULTS

A. LOW-TEMPERATURE EQUILIBRIA - - THE SOLID STATE SECTION AT 1400°C

The solid state section at 1400°C (Figure 9) was determined by studying the X-ray films and by metallography of 31 samples which had been heat-treated at 1400°C for 100 hours. Most of the samples were pieces of larger samples that had been used in melting point determinations, although several samples of 50 At.% boron on the titanium-rich side were hot pressed and only arc-melted prior to the heat-treatment. Figure 8 shows the compositional location of these samples.

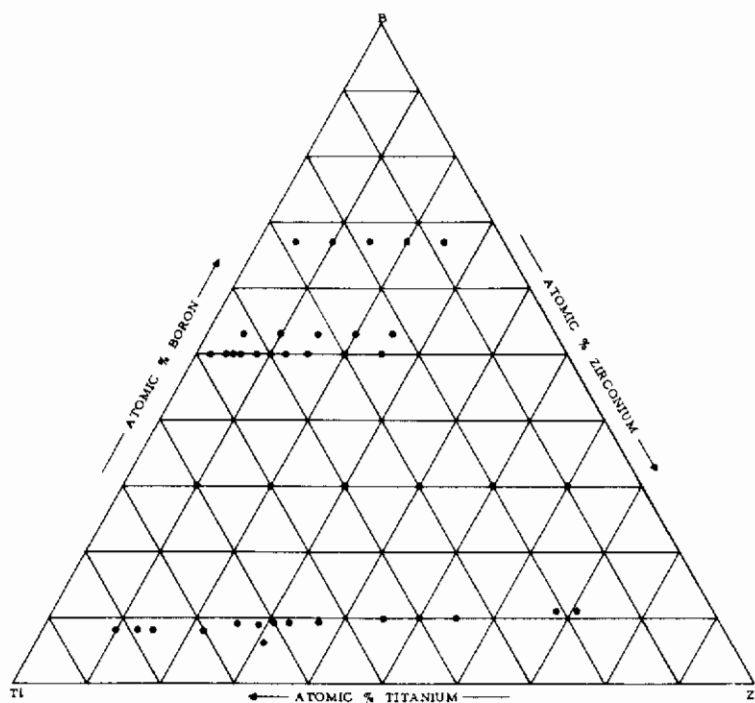


Figure 8. Composition of Alloys Investigated for the Solid State Section at 1400°C.

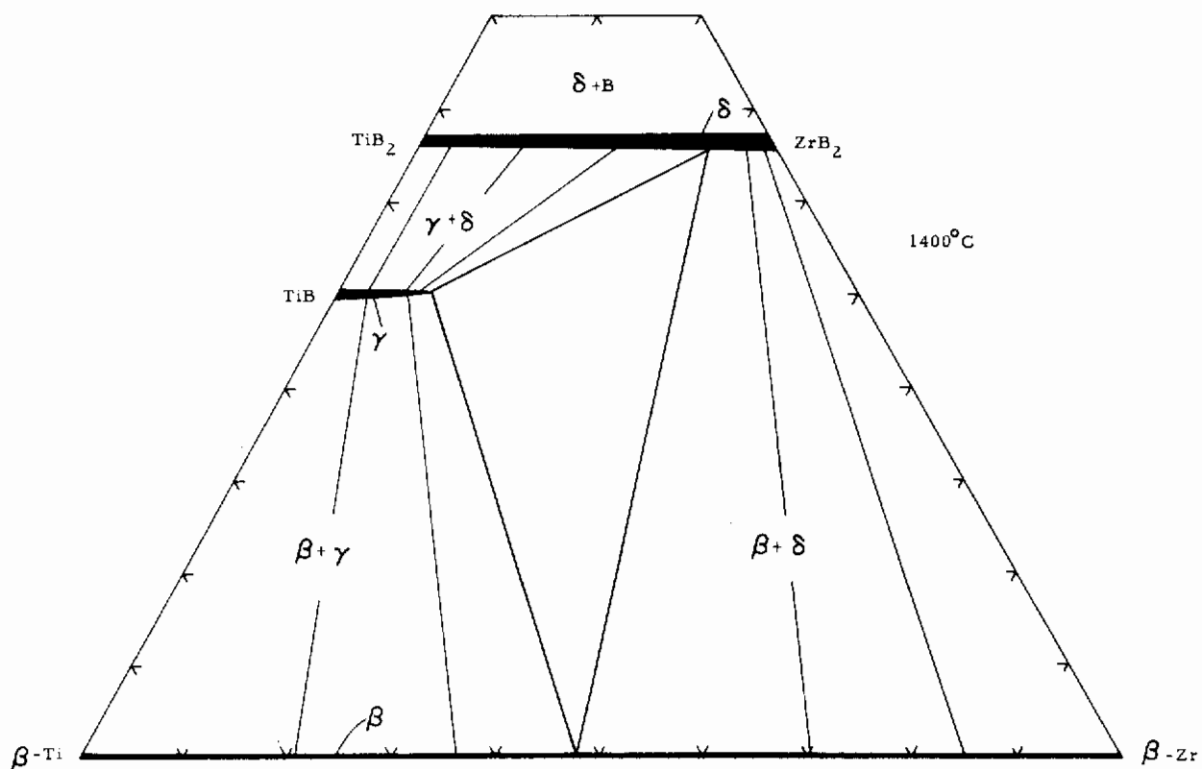


Figure 9. Isothermal Section at 1400°C.

Samples of composition (all compositions designated in the following manner are in atomic percent) Ti-Zr-B: 79-13-8, 60-31-9, 50-20-30, and 60-10-30 were two-phased, metal and metal monoboride (see for example Figure 10) the large dark grains in Figure 10, are primary metal monoboride in a metal-metal monoboride eutectic. Figure 11 shows the

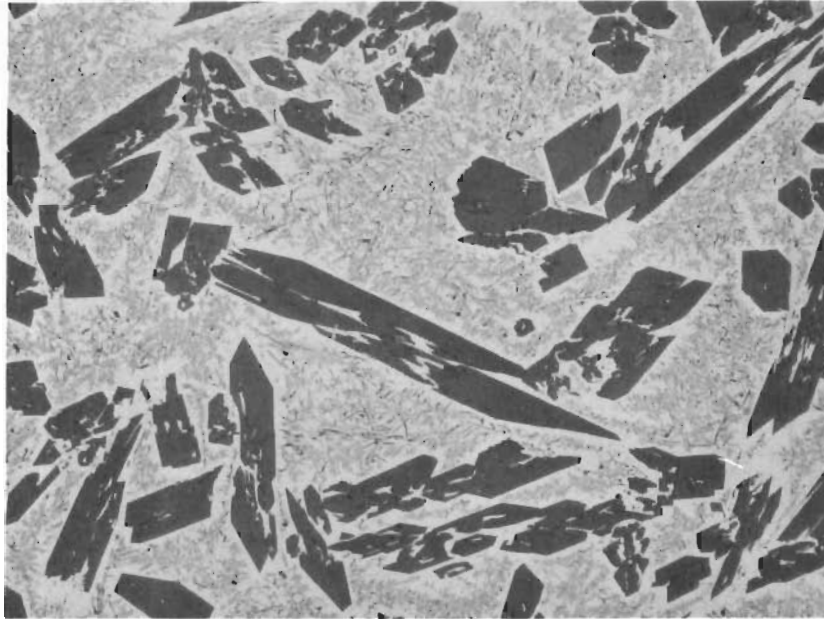


Figure 10. Primary Monoboride and Monoboride-Metal Eutectic. Ti-Zr-B: 60-10-30.

X100

metallography of a sample whose composition Ti-Zr-B: 79-13-8 is very near the eutectic trough (See Figure 21). This sample is two-phased, metal monoboride and metal.

On the zirconium-rich side, samples of composition Ti-Zr-B: 40-50-10, 21-68-11, 20-50-30, and 10-60-30 were found to be two-phased, metal and metal diboride (e.g. Figures 12 and 13). Again, one of these was of a composition very near the eutectic trough (see Figure 14). Samples of composition Ti-Zr-B: 40-30-30, 35-15-50, 30-20-50, 25-25-50, and 22-25-53 were found to be three-phased (Figures 15, 16, and 17): metal, monoboride, and diboride,

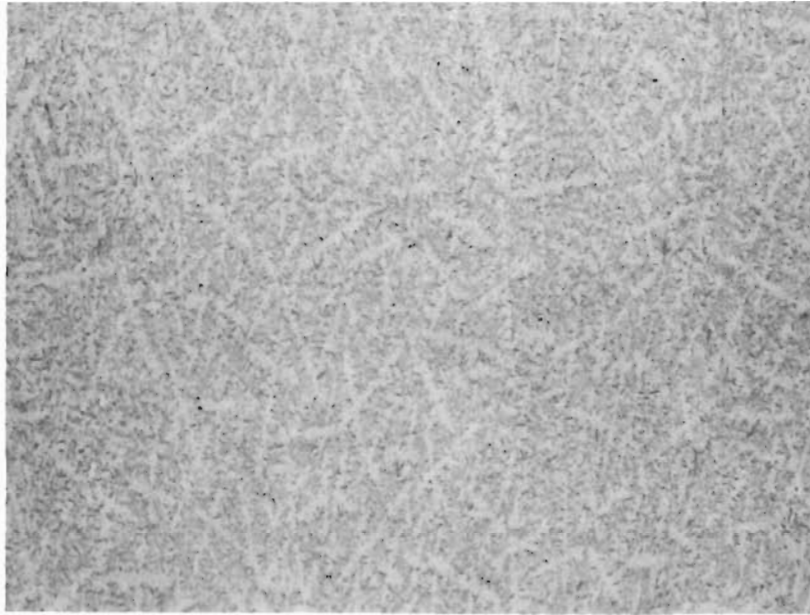


Figure 11. Micrograph of Ti-Zr-B (79-13-8) Alloy
Near the Metal-Metal Monoboride Eutectic
Trough.

X300

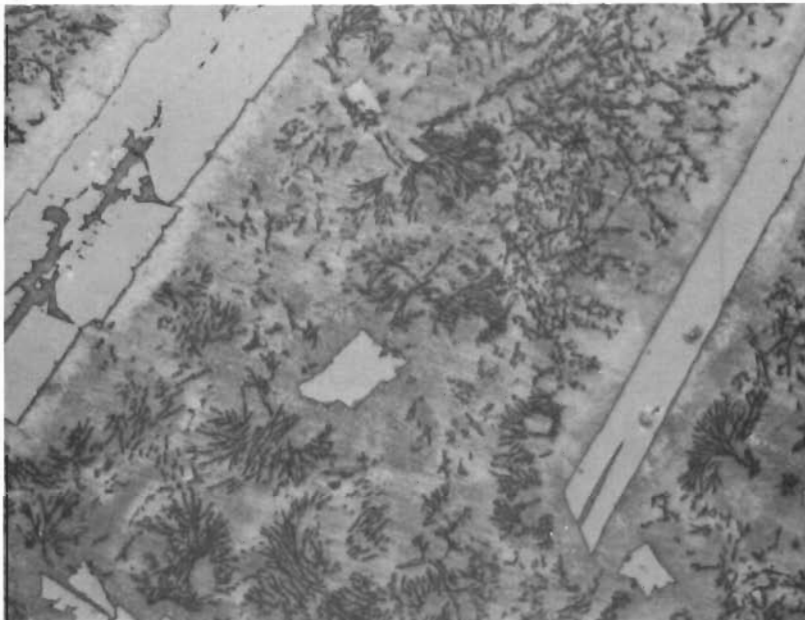


Figure 12. Micrograph of an Arc-Melted Ti-Zr-B
(20-50-30) Alloy.

X500

Diboride **Grains** and Diboride-Metal Eutectic in
Metal Matrix.

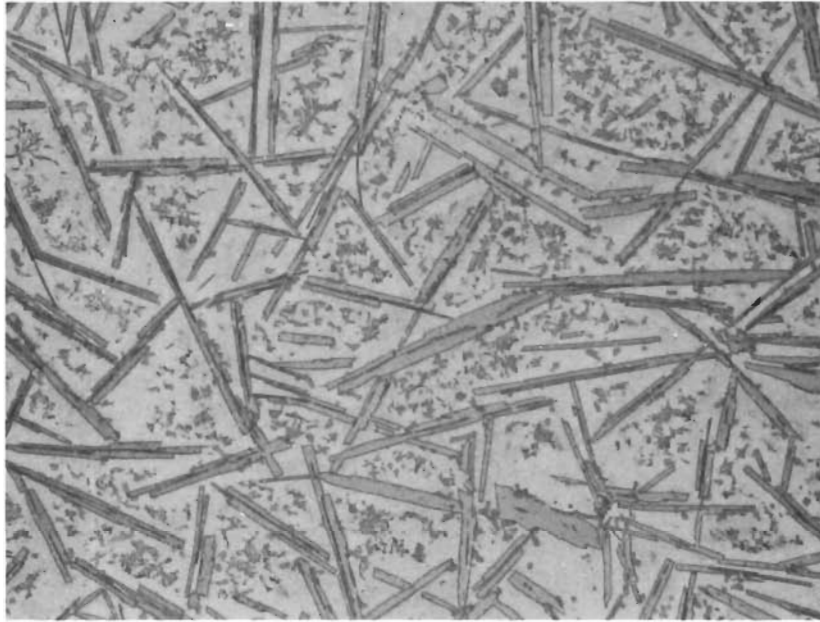


Figure 13. Micrograph of an Arc-Melted, Ti-Zr-B
(10-60-30) Alloy.

X150

Diboride Grains and Diboride-Metal Eutectic in the
Metal Matrix.

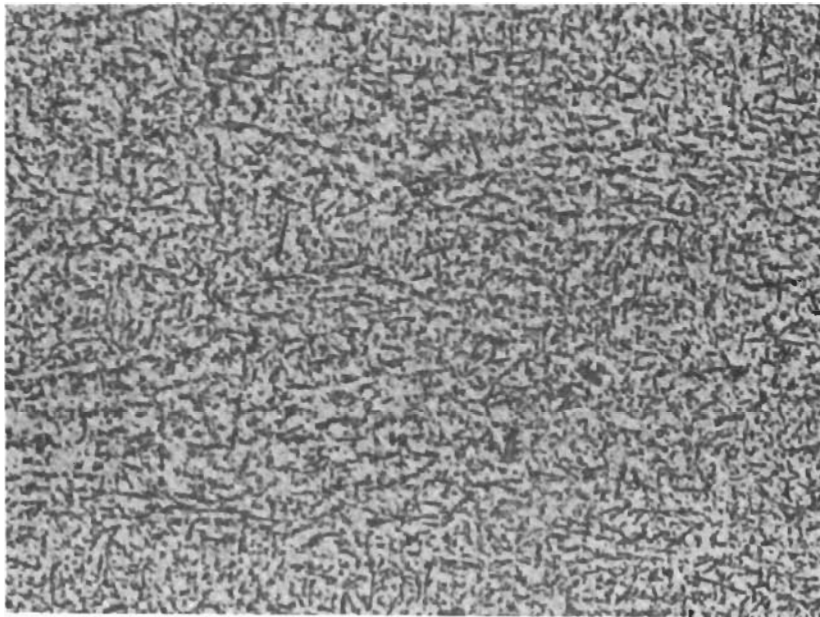


Figure 14. Micrograph of Ti-Zr-B (21-68-11) Alloy.

X250

Diboride-Metal Eutectic.

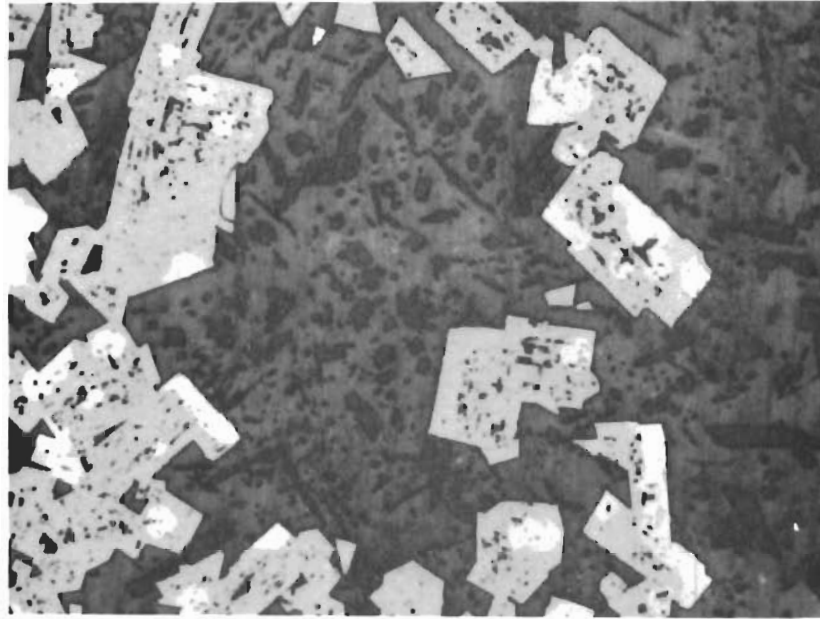


Figure 15. Micrograph of Ti-Zr-B (40-30-30) Alloy.

X625

Diboride (Light Colored Grains) and Monoboride
(Dark Grains) in Metal Matrix.

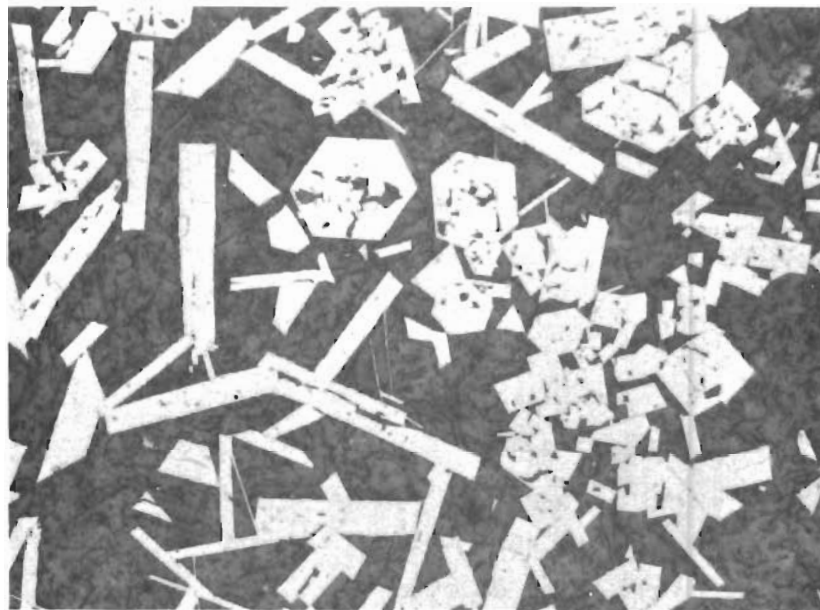


Figure 16. Micrograph of Ti-Zr-B (25-25-50), Alloy.

X300

Diboride and Monoboride in Metal Matrix.

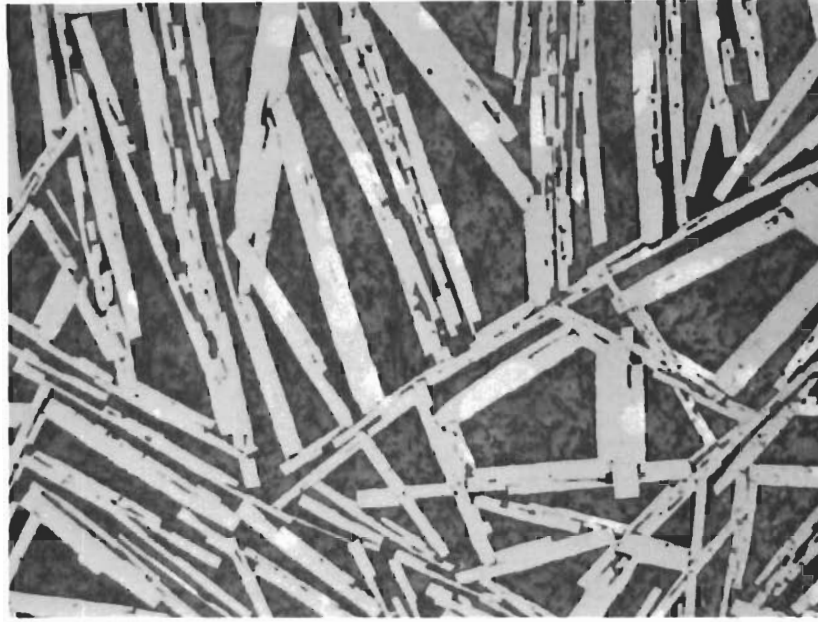


Figure 17. Micrograph of an Arc-Melted Ti-Zr-B (22-25-53) X425 Alloy.

Diboride and Monoboride in Metal Matrix.

although the latter two samples had very small quantities of the metal monoboride phase present. Samples at 45-5-50 and 40-10-50 (Figure 18) were also three-phased, but this was due to non-equilibrium conditions arising from their heat-treatment. In these samples, large macroscopic grains of diboride are in equilibrium with the liquid at temperatures above 2200°C, and when these samples are cooled, the peritectic reaction occurs forming the monoboride around the diboride grains, thus shutting off the diboride grain from the surrounding liquid (and at lower temperatures, metal) phase. Thus, the peritectic reaction is diffusion limited and proceeds very slowly at temperatures below the solidus. When the past heat-treatment history of the sample was such as to form only small diboride grains, the samples at these compositions show little or no diboride phase present. Figure 18 shows clearly the peritectic reaction just described. Other samples near in composition to titanium diboride were studied, and the following results obtained. X-ray films of samples of composition Ti-Zr-B: 50-0-50, 48-2-50, 46-4-50, 45-5-50, 44-6-50, 42-8-50, 40-10-50, 38-12-50, and 35-15-50 were examined,

and the monoboride phase showed changing lattice parameters for the first six samples and constant lattice parameters for the last three samples. Due to non-equilibrium conditions in the samples, the X-ray films were not actually measured and lattice parameters calculated from the measurements, but rather the θ values for a few front lines on the films (since the back lines were extremely faint and diffuse) were compared. The result of these evaluations is that the maximum zirconium exchange in titanium monoboride was found to be 9 At.% zirconium (± 1 At.%).

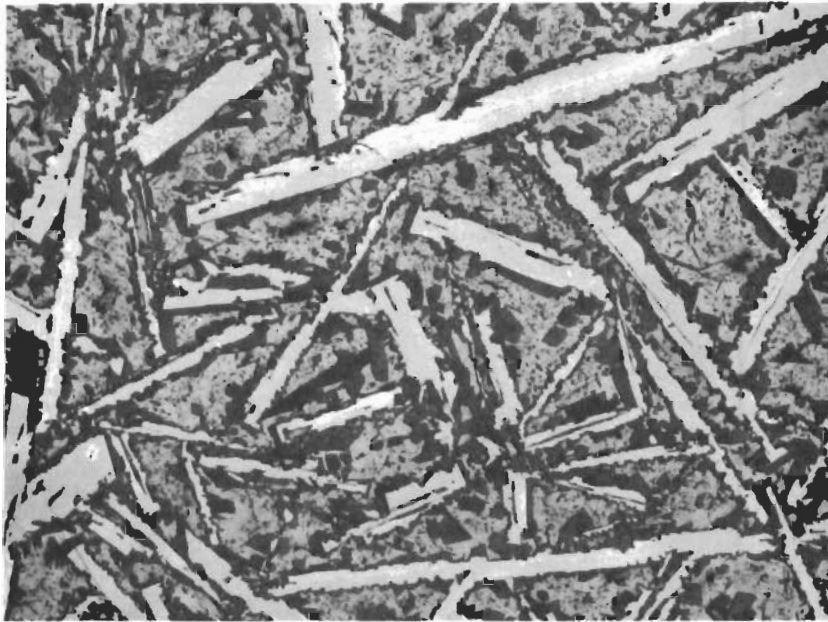


Figure 18. Micrograph of Ti-Zr-B (40-10-50) Alloy

X130

For the solid state section, five ternary diboride samples were prepared, melted, and then heat-treated with the rest of the samples at 1400°C for 100 hours. The X-ray films of these samples were measured, and lattice parameters were calculated and plotted (Figure 19, which also shows the lattice parameters measured by other investigators). The lattice parameters of the diboride solid solution very closely follow Vegard's law. The samples were of composition Ti-Zr-B: 28-5-67, 23-10-67, 18-15-67, 13-20-67, and 8-25-67. The X-ray films showed no other phases to be present, but under metallographic examination, although all samples appeared to be nearly single

phased, small quantities of metal and monoboride phases were found in the grain boundaries (Figure 20). This is undoubtedly due to the extremely narrow range of homogeneity. The θ values of the 212 line of the diffraction patterns of all the samples containing sufficient quantity of diboride to give intense enough diboride lines on an X-ray film were compared, and yielded the following results: Samples in the three-phased region (i.e., samples whose metallography showed three phases, and whose lattice parameters did not vary with varying composition) contained a diboride of composition very near Ti-Zr-B: 7-27-66, while samples in the two-phased region, monoboride, and diboride, contained titanium richer diborides; samples in the two-phased region, diboride and metal, contained zirconium-richer diborides.

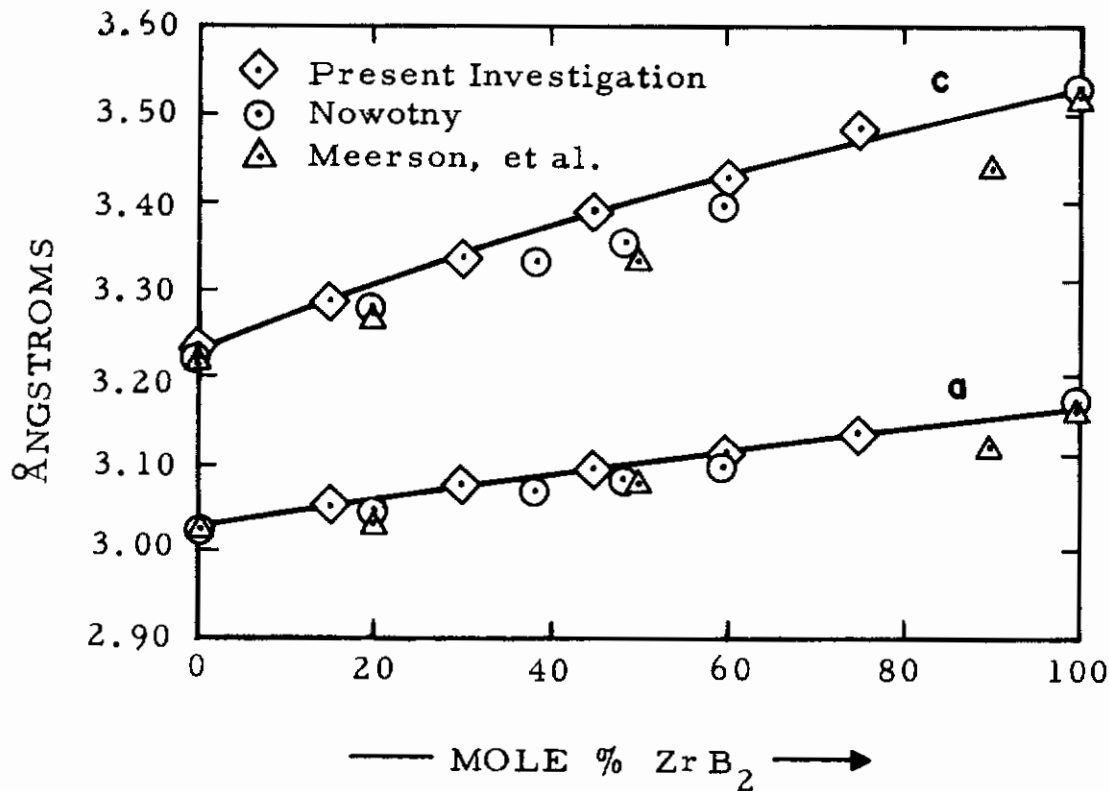


Figure 19. Lattice Parameters of Ternary Diboride Alloys Equilibrated at 1400°C.

The compositions of the three phases in equilibrium with each other at 1400°C have thus been found to be: metal phase at Ti-Zr-B: 51-51-48-1, monoboride at 41-9-50, and diboride at 7-27-66 (Figure 9). The greatest uncertainty is in the composition of the metal phase which was determined from the composition of the other two phases and the metallography; hence, the composition lies between 59-40-1 and 44-55-1, leaving a possible uncertainty in composition of ± 8 At.%. The uncertainty of the compositions of the monoboride and the diboride phases is estimated ± 1 At.% and ± 2 At.% respectively.

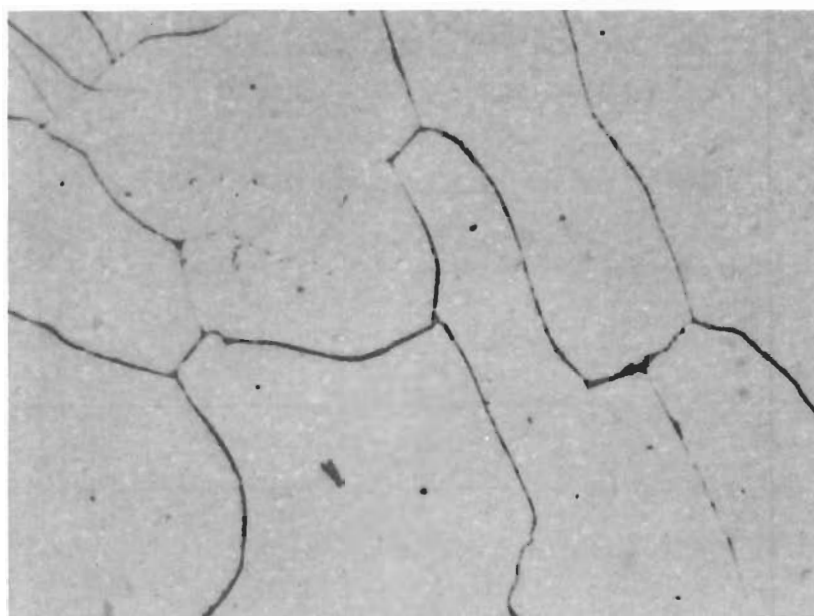


Figure 20. Micrograph of Ti-Zr-B (28-5-67) Alloy.

X850

Diboride Grains with Metal in Grain Boundaries

Comparison of diboride lattice parameters in the two-phased regions, metal and diboride, and monoboride and diboride, were also used to estimate tie lines in these regions. The tie lines in the two-phase region, metal and monoboride, were not nearly so well established since both the metal and the monoboride lines were diffuse because non-equilibrium conditions prevailed in the samples in this region.

B. HIGH-TEMPERATURE EQUILIBRIA

Minimum melting occurs in the ternary (Figures 21 and 22). Ten samples were prepared with compositions very near where the eutectic trough was expected to lie. Since a minimum occurs in the solidus curve of the metal binary at about 34 At.% zirconium, ternary samples were prepared with more samples near this binary composition. The results of the incipient melting point determinations of these samples are shown in Figure 21. Metallographic investigation of these samples was performed (Figures 11, 14) and the results are shown in Figure 21.

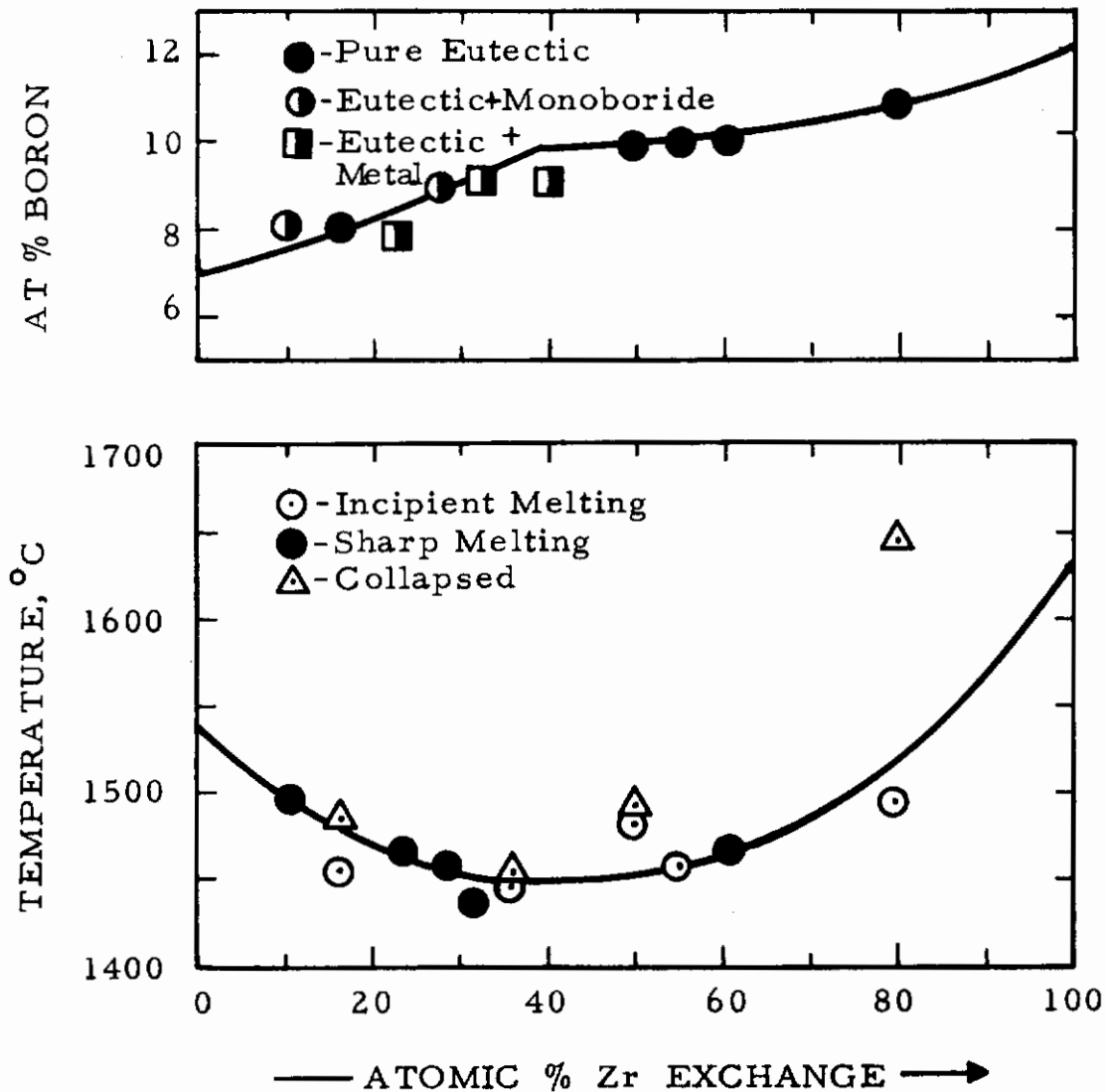


Figure 21. Melting Points and Position of Metal-Rich Eutectic Trough.

A four-phase reaction occurs at 1450°C (Figure 23). The compositions of the four phases participating in the four-phase reaction (Table 1) were estimated with the aid of the 1400°C section and the plot of melting points along the eutectic trough (Figures 8, 21). With increasing temperature, a Class II four-phase reaction results (Figure 23) from the merging of the adjacent three-phase fields $L + \beta + \gamma$, and $\beta + \gamma + \delta$:

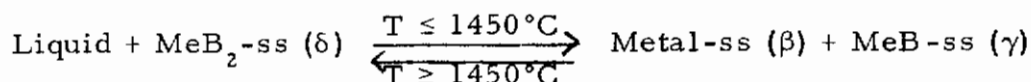


Table 1. Composition of the Phases Participating in the Four-Phase Reaction at 1450°C.

Phase	Concentrations, At. %		
	Ti	Zr	B
β -Ti, Zr (β)	50	49	1
(Ti, Zr)B (γ)	41	9	50
(Ti, Zr)B ₂ (δ)	7	27	66
Liquid	52	37	11

With increasing temperature the two three-phase fields $L + \gamma + \delta$ and $L + \beta + \delta$ and vanish into the appropriate binaries. One can see by examination of the three-phase field at 1400°C and the melting points along the eutectic trough, that the four-phase reaction will occur at a temperature very slightly in excess of the minimum melting temperature (i.e., less than five degrees) of the eutectic trough.

The results of the melting point investigations are listed in Table 2. From these data, as well as from the binary diagrams, the solidus and to a lesser degree the liquidus surfaces were determined. The results are made more useful in the form of a plot of liquidus projections in Figure 24. In some instances, melting points observed in samples near the titanium monoboride region were too low due to incomplete reaction of the starting components. Therefore, the melting point of the starting materials disguised the true melting temperatures.

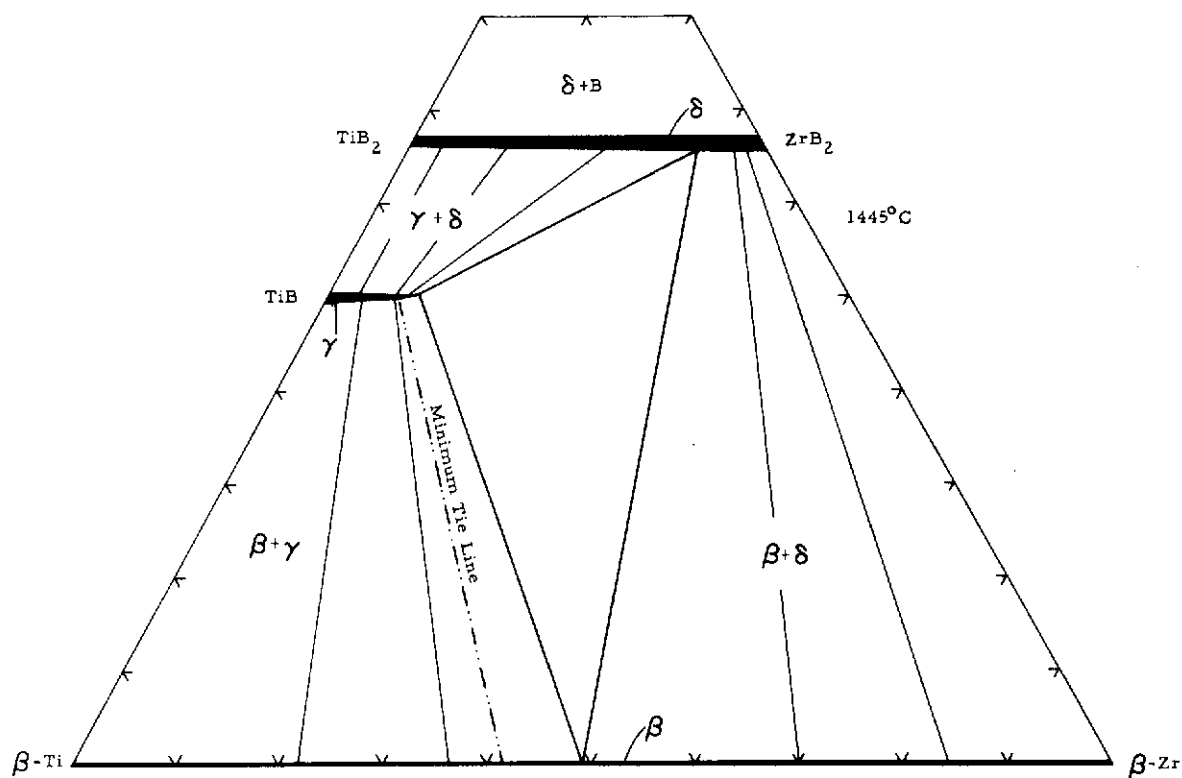


Figure 22. Isothermal Section at 1445°C.

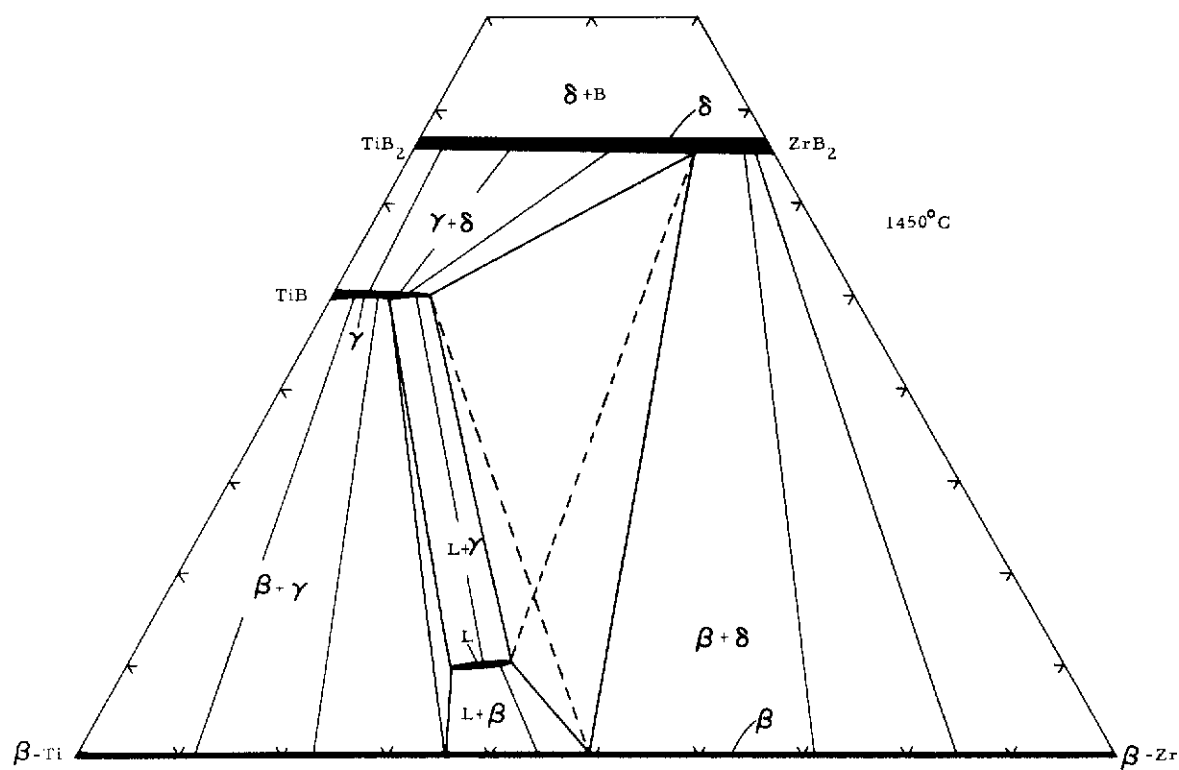


Figure 23. Isotherm at 1450°C.

[Four-Phase Reaction Plane ($L + \delta \rightleftharpoons \beta + \gamma$)]

Table 2. Results of Melting Point Investigations

Nominal Compositions in At. %			Melting Temperatures °Centigrade		Melting Behavior	Phases Present
Ti	Zr	B	Incipient	Collapsing		
63	31	6	1465	1505		Me + Me-MeB eutectic
82	10	8	1496	1496	Sharp	MeB + Me-MeB eutectic
75	15	8	1455	1486	Heterogeneous	Me-MeB eutectic
70	72	8	1465	1465	Sharp	Me + Me-MeB eutectic
65	26	9	1455	1455	Sharp	MeB + Me-MeB eutectic
62	29	9	1435	1435	Sharp	MeB + Me-MeB eutectic
60	31	9	1455	1485	Heterogeneous	Me + Me-MeB eutectic
58	33	9	1445	1445	Sharp	n.d.
54	37	9	1455	1500	Heterogeneous	Me + Me-MeB eutectic
45	45	10	1480	1490	Heterogeneous	Me + MeB + MeB ₂
35	55	10	1465	-	Slightly Heterog.	Me-MeB ₂ eutectic
18	71	11	1494	1646	Heterogeneous	Me-MeB ₂ eutectic
60	10	30	1465	1495	Heterogeneous	Me + MeB
50	20	30	1491	1536	Heterogeneous	Me + MeB
40	30	30	1485	1556	Heterogeneous	Me + MeB + MeB ₂ (1)
30	40	30	1495	1582	Heterogeneous	Me + MeB + MeB ₂
20	50	30	1448	1495	Heterogeneous	MeB ₂ + Me
10	60	30	1440	1567	Heterogeneous	MeB ₂ + Me
40	10	50	2211	2580	Very Heterog.	Me + MeB + MeB ₂ (2)
35	15	50	2086	2225	Very Heterog.	Me + MeB + MeB ₂ (2)
30	20	50	2149	2231	Very Heterog.	Me + MeB + MeB ₂
25	25	50	2179	2713	Very Heterog.	Me + MeB + MeB ₂
22	25	53	2220	2548	Very Heterog.	Me + MeB + MeB ₂
27	20	53	-	1985	Very Heterog.	Me + MeB + MeB ₂

Table 2 (Continued)

Nominal Compositions in At. %			Melting Temperatures °Centigrade		Melting Behavior	Phases Present
Ti	Zr	B	Incipient	Collapsing		
32	15	53	1822	1985	Very Heterog.	Me + MeB + MeB ₂
37	10	53	2200	2415	Very Heterog.	Me + MeB + MeB ₂ + carbide
42	5	53	2046	2333	Very Heterog.	Me + MeB + MeB ₂ + carbide
30	2.5	67.5	2780	2905	Heterogeneous	n.d.
25	8.5	66.5	2702	2750	Fairly Sharp	n.d.
20	12.5	67.5	2700	2835	Heterogeneous	n.d.
20	14	66	2952	2994	Fairly Heterog.	n.d.
17	16	67	2804	2804	Heterogeneous	n.d.
14.5	19	66.5	2680	2910	Heterogeneous	n.d.
10.5	23	66.5	2680	2930	Fairly Sharp	n.d.
4	28	68	3025	3025	Heterogeneous	n.d.

(1) amount of MeB is small

(2) peritectic reaction not completed

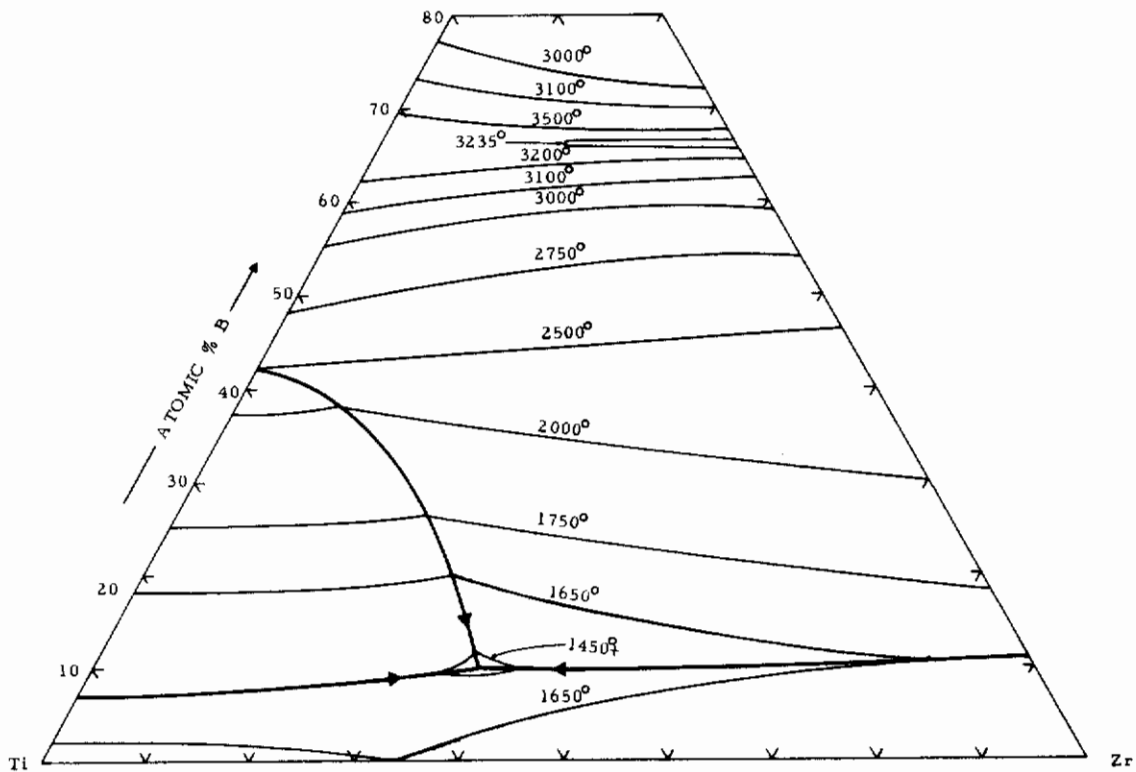


Figure 24. Plot of Liquidus Projections.

The formation of a continuous series of solid solutions of the (titanium, zirconium) diborides has been established by other investigators (6, 7, 8, 9, 10), and no significant departures from their results were found in this investigation. Nine ternary samples approximately in the 66 At. % boron range were melted in the Pirani melting point furnace. They were selectively heat-treated and studied by X-ray and metallographic techniques. A very slight deviation from Vegard's law is seen (Figure 19). The melting points are plotted in Figure 25. An example of the metallography (Figure 20 shows nearly single phase diboride grains. Actually, many of the samples showed small amounts of other phases in the grain boundaries. This is indicative of the narrow range of homogeneity, which makes the accurate determination of melting point temperatures very difficult.

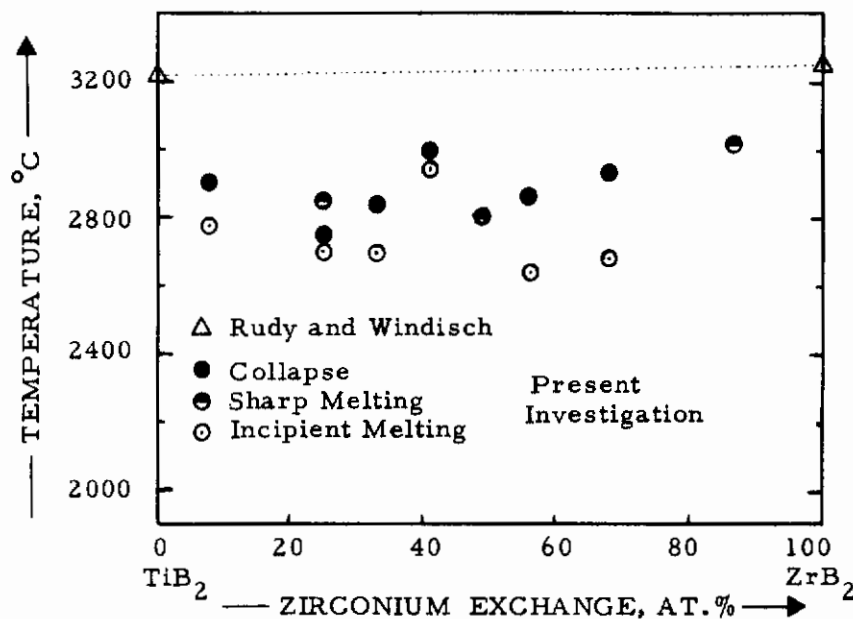


Figure 25. Observed Melting Temperatures of Ternary Diboride Alloys.

The results of the melting point determinations of samples in the diboride series of solid solutions were somewhat disappointing. Great experimental difficulty was experienced when melting these samples. The major problem is the narrow range of homogeneity mentioned above. Slight shifts in composition or small inhomogeneities in the sample cause the observable incipient melting temperature to be lower (even by hundreds of degrees) than that of the true diboride solid solution. The melting point determinations were also made more difficult by the appearance of smoke upon heating and by the formation of tiny crystals on the surface of the specimen.

Figures 26 through 40 depict the isothermal sections of the Ti-Zr-C system in the temperature range 1400° to 3225°C. Three of these figures appeared earlier in the text.

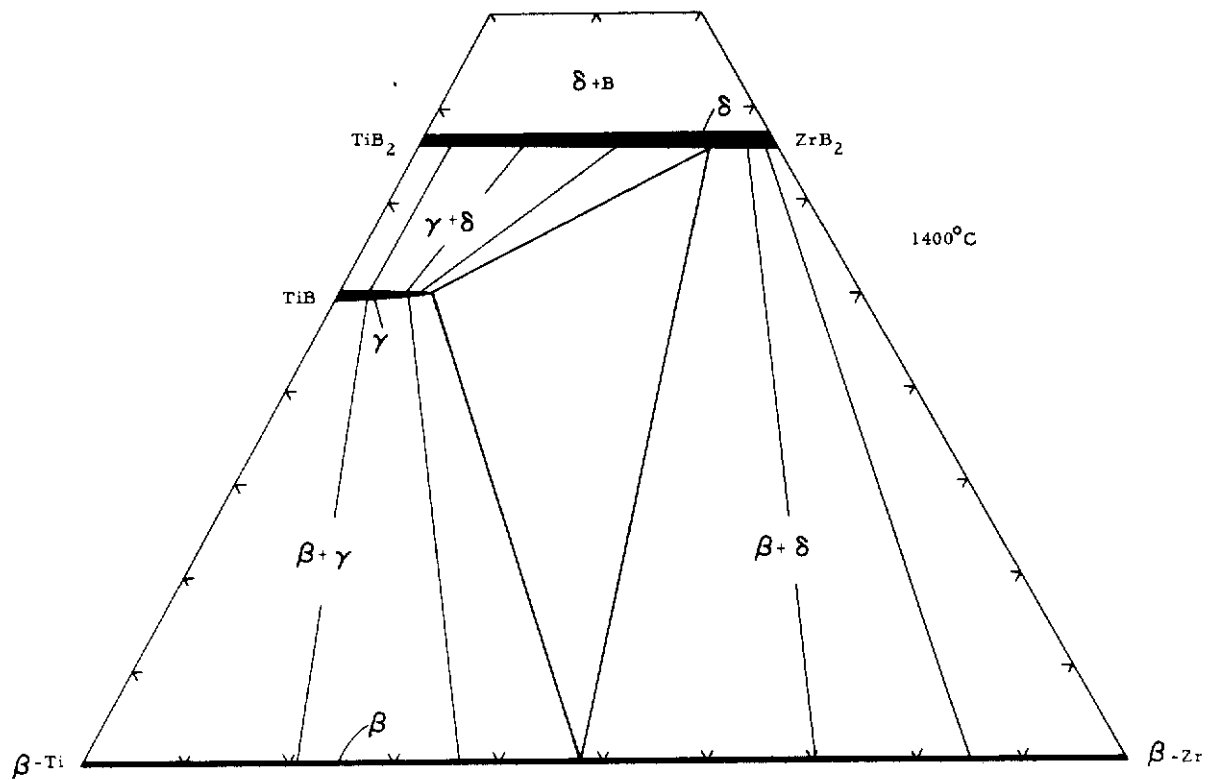


Figure 26. Isothermal Section at 1400°C.

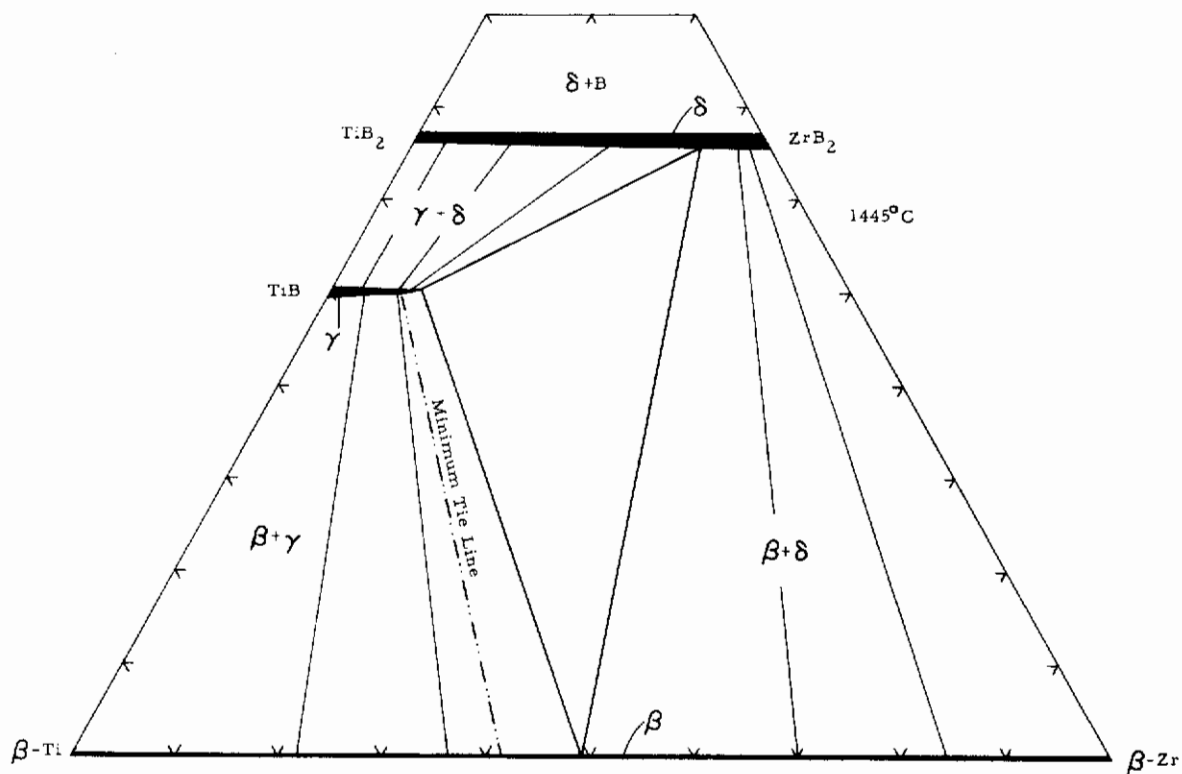


Figure 27. Isothermal Section at 1445°C.

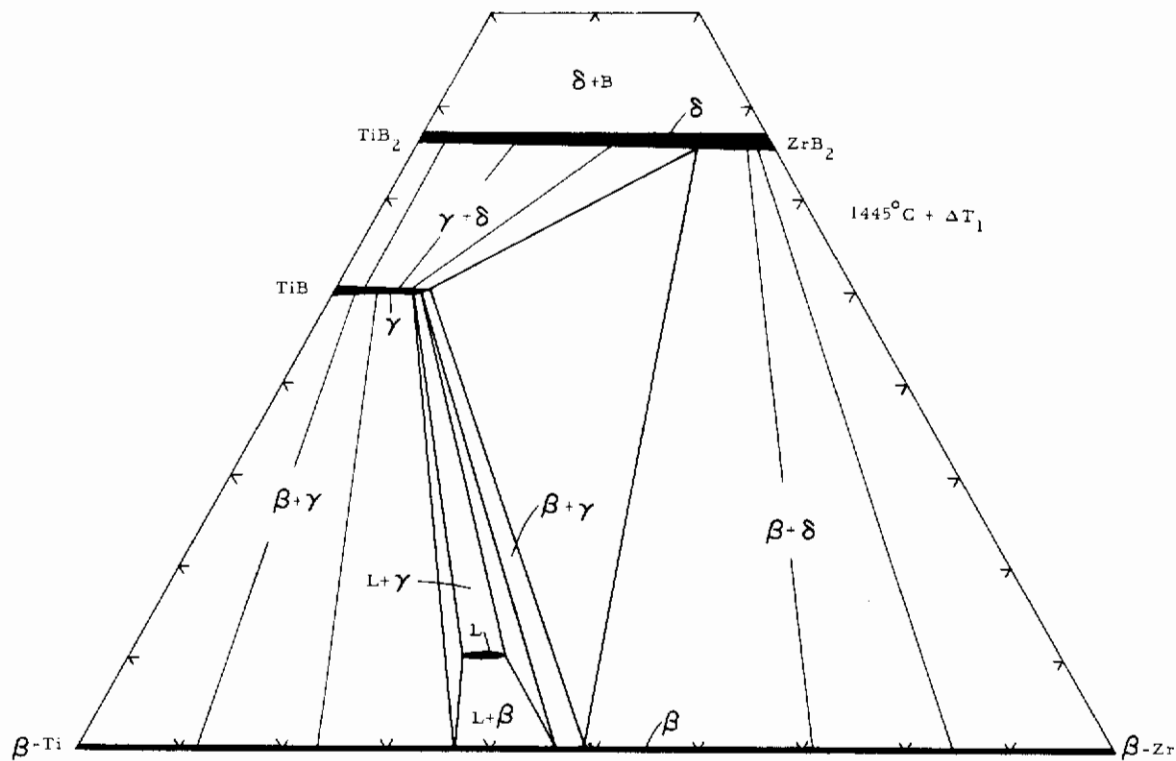


Figure 28. Isothermal Section at 1445°C + ΔT_1 .

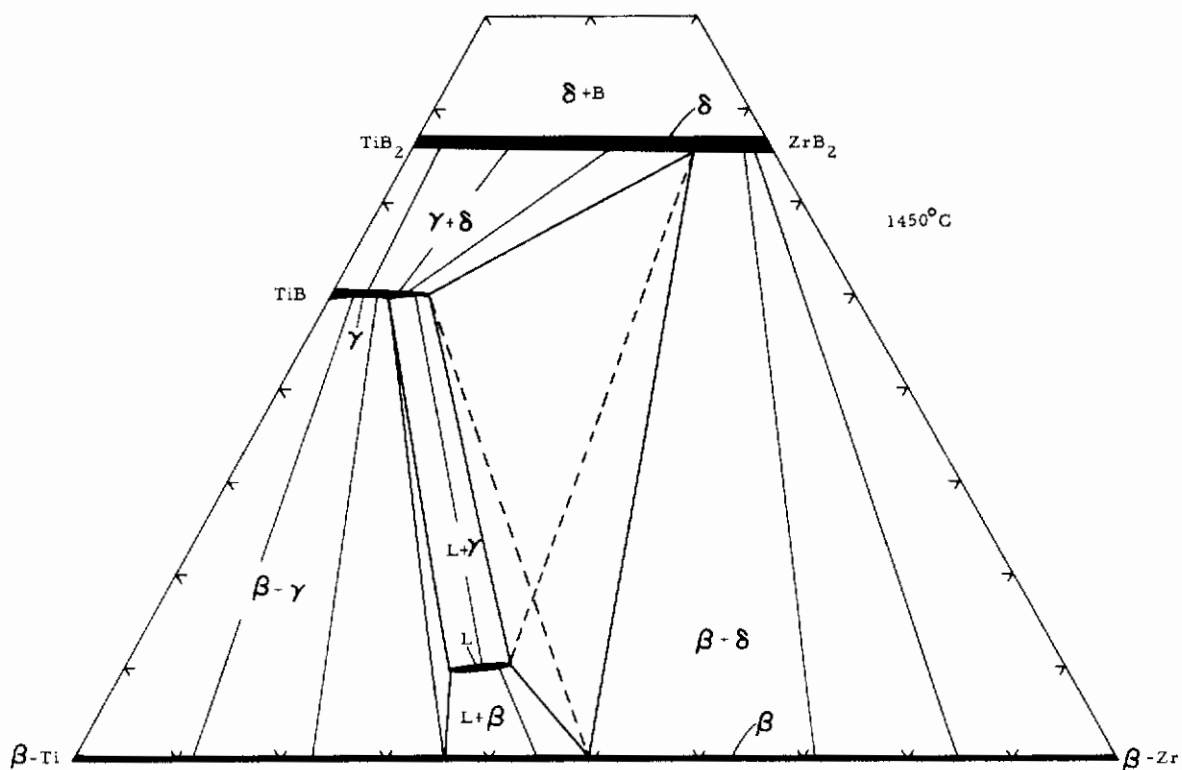


Figure 29. Isothermal Section at 1450°C.
[Four-Phase Reaction ($L + \delta \rightleftharpoons \beta + \gamma$)]

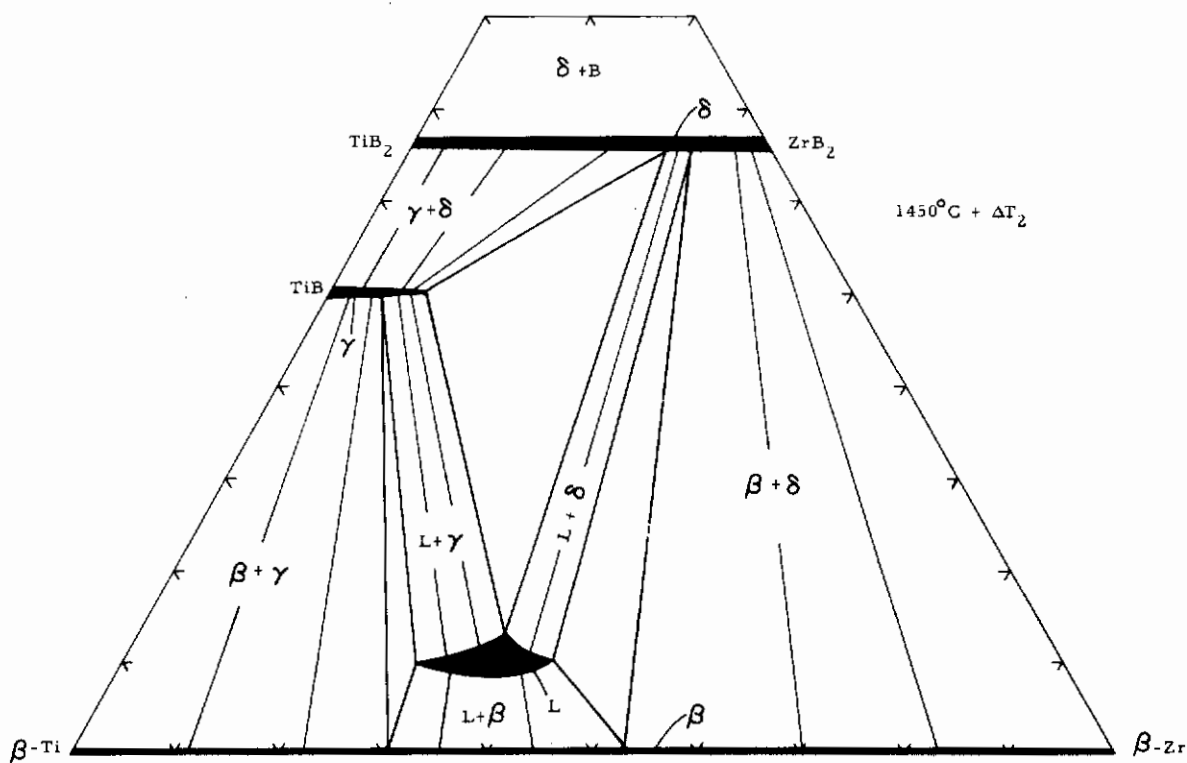


Figure 30. Isothermal Section at 1450°C + ΔT_2 .

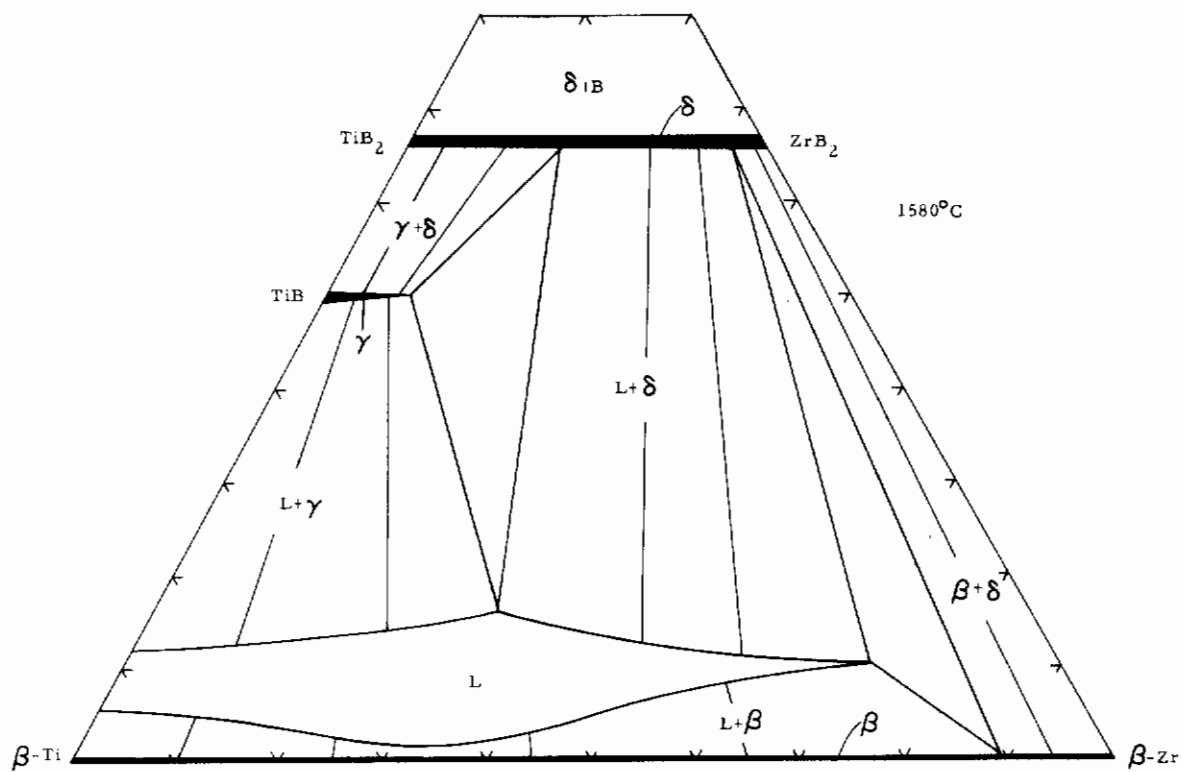


Figure 31. Isothermal Section at 1580°C.

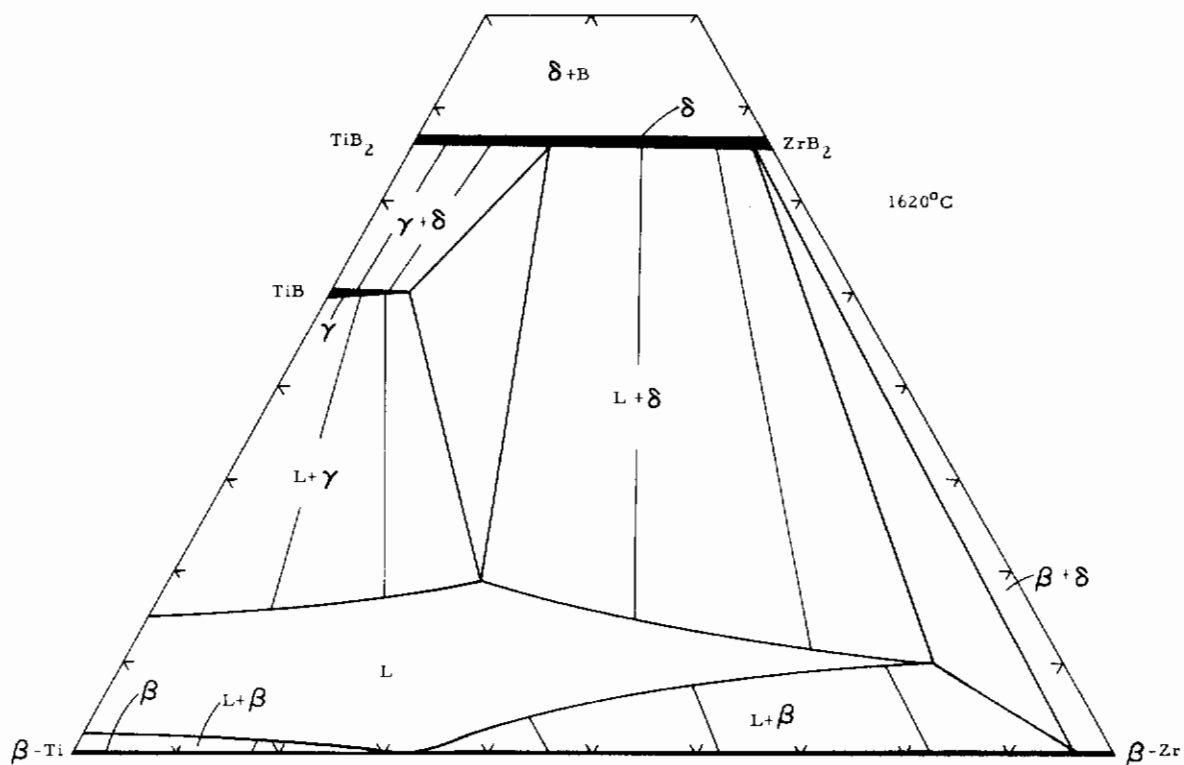


Figure 32. Isothermal Section at 1620°C.

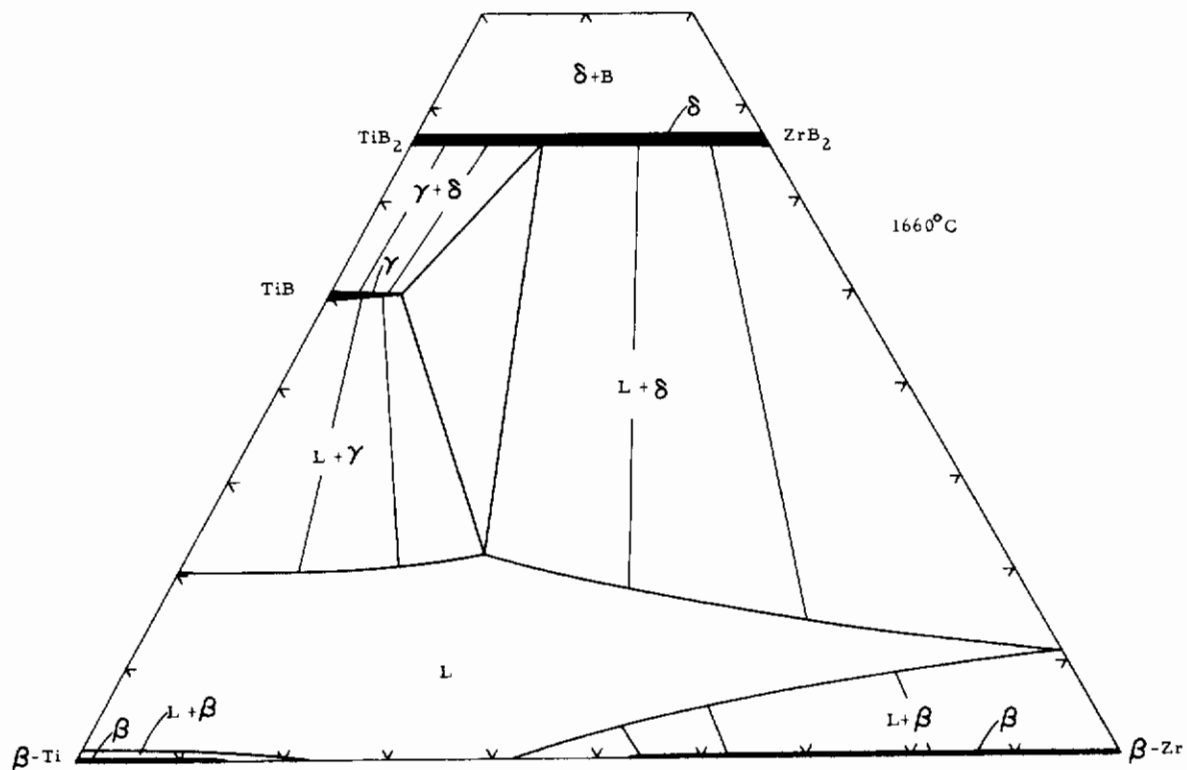


Figure 33. Isothermal Section at 1660°C.

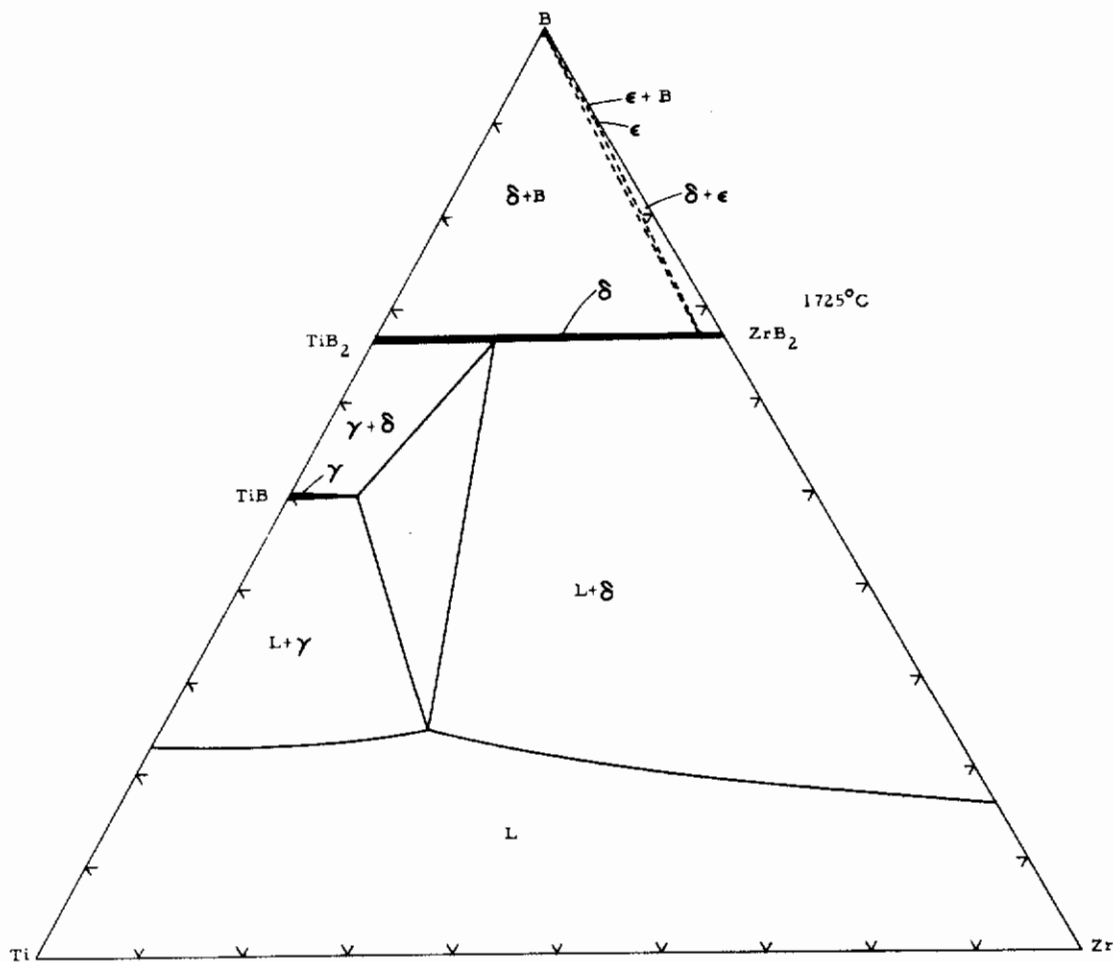


Figure 34. Isothermal Section at 1725°C.

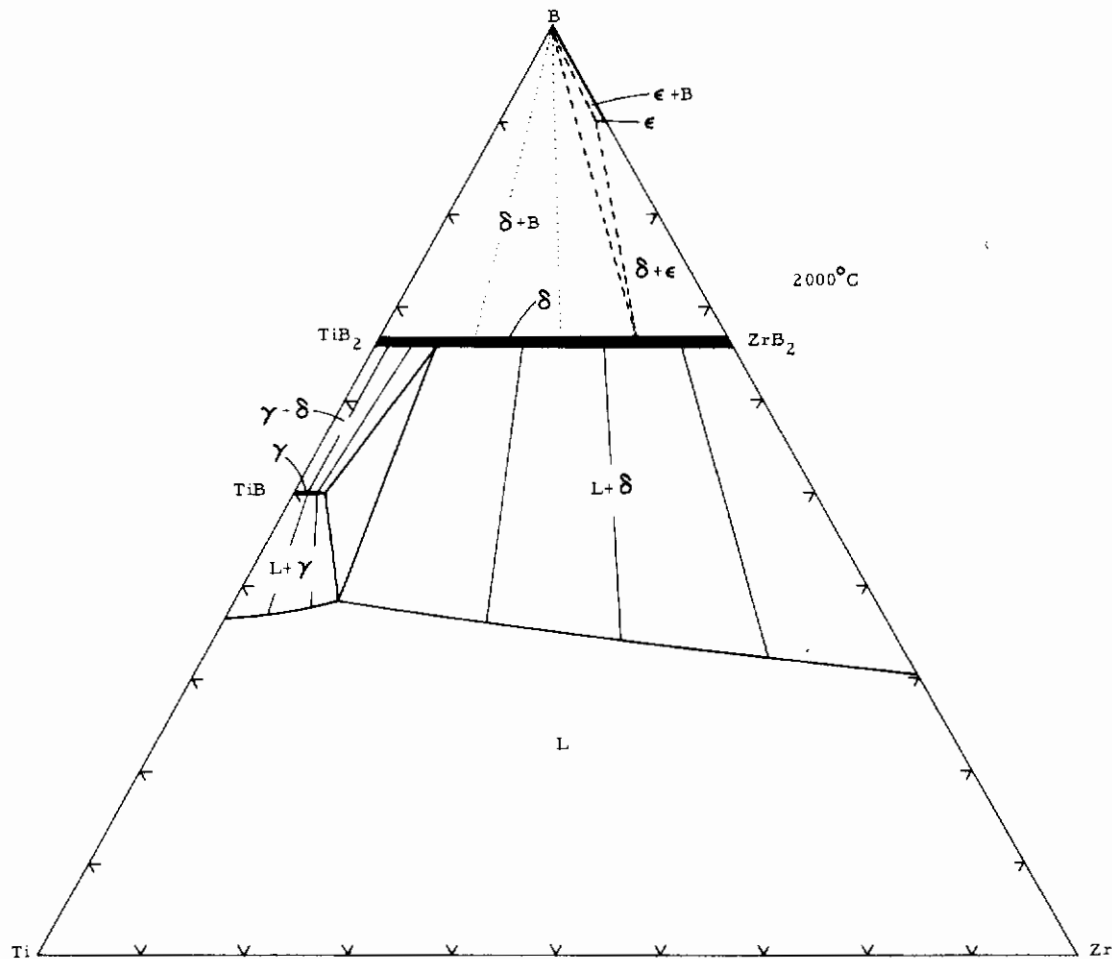


Figure 35. Isothermal Section at 2000°C.

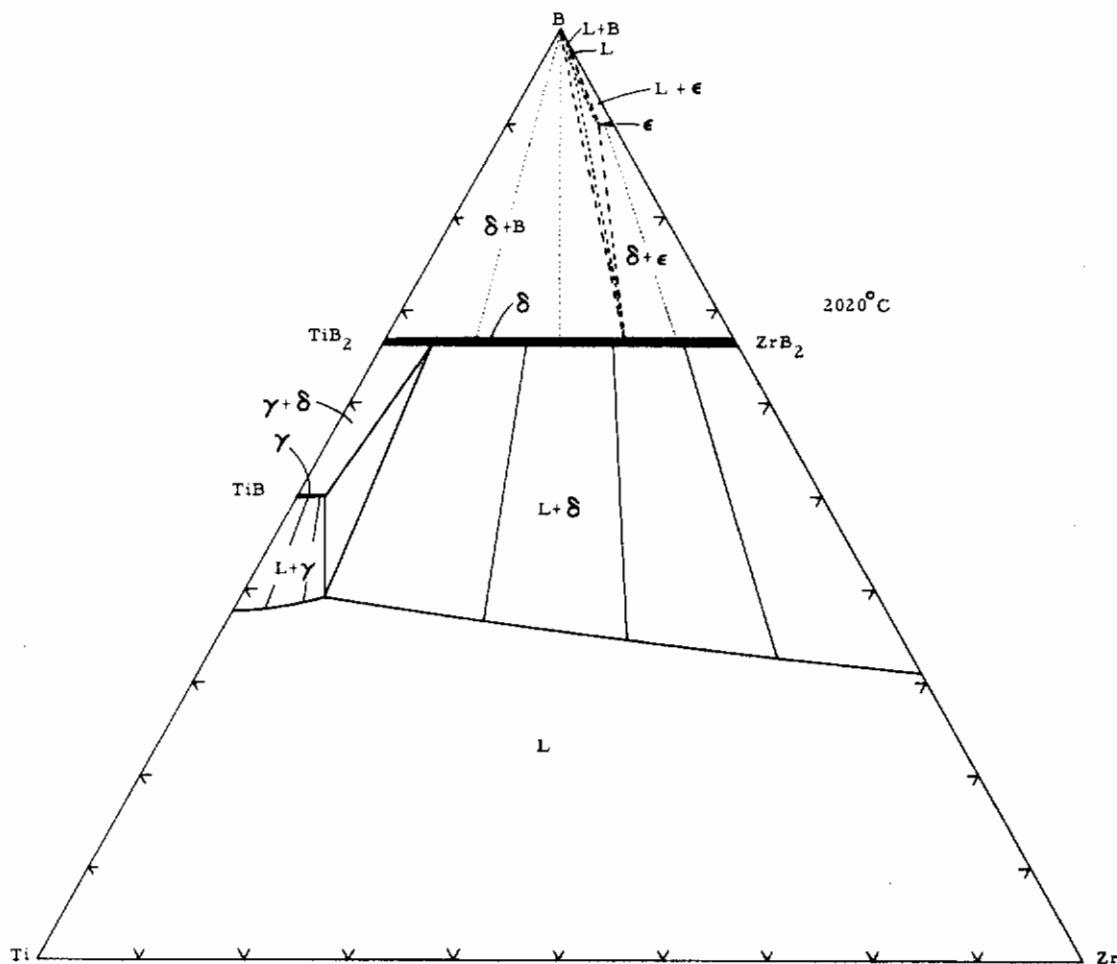


Figure 36. Isothermal section at 2020°C.

[Four-Phase Reaction ($L + \delta \rightleftharpoons \epsilon + B$)], Estimated.

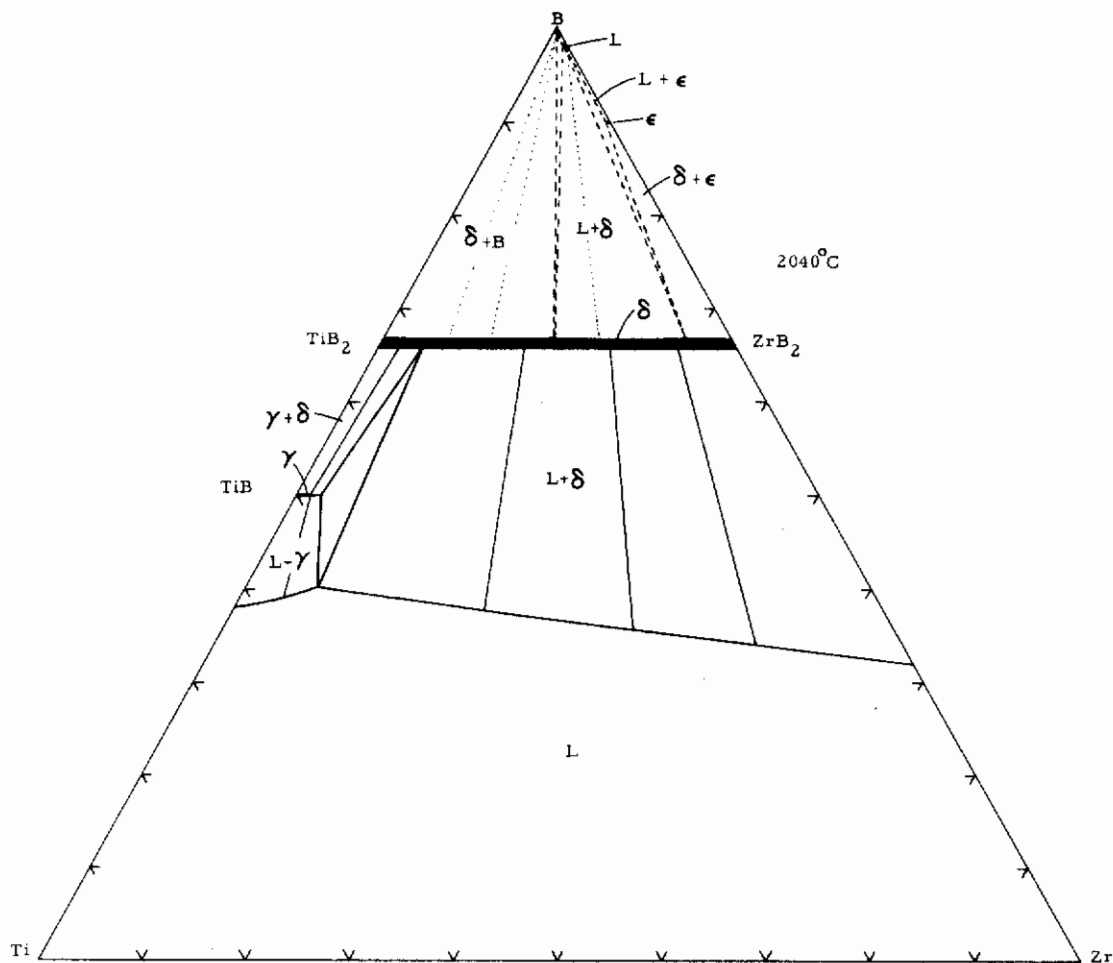


Figure 37. Isothermal Section at 2040°C.

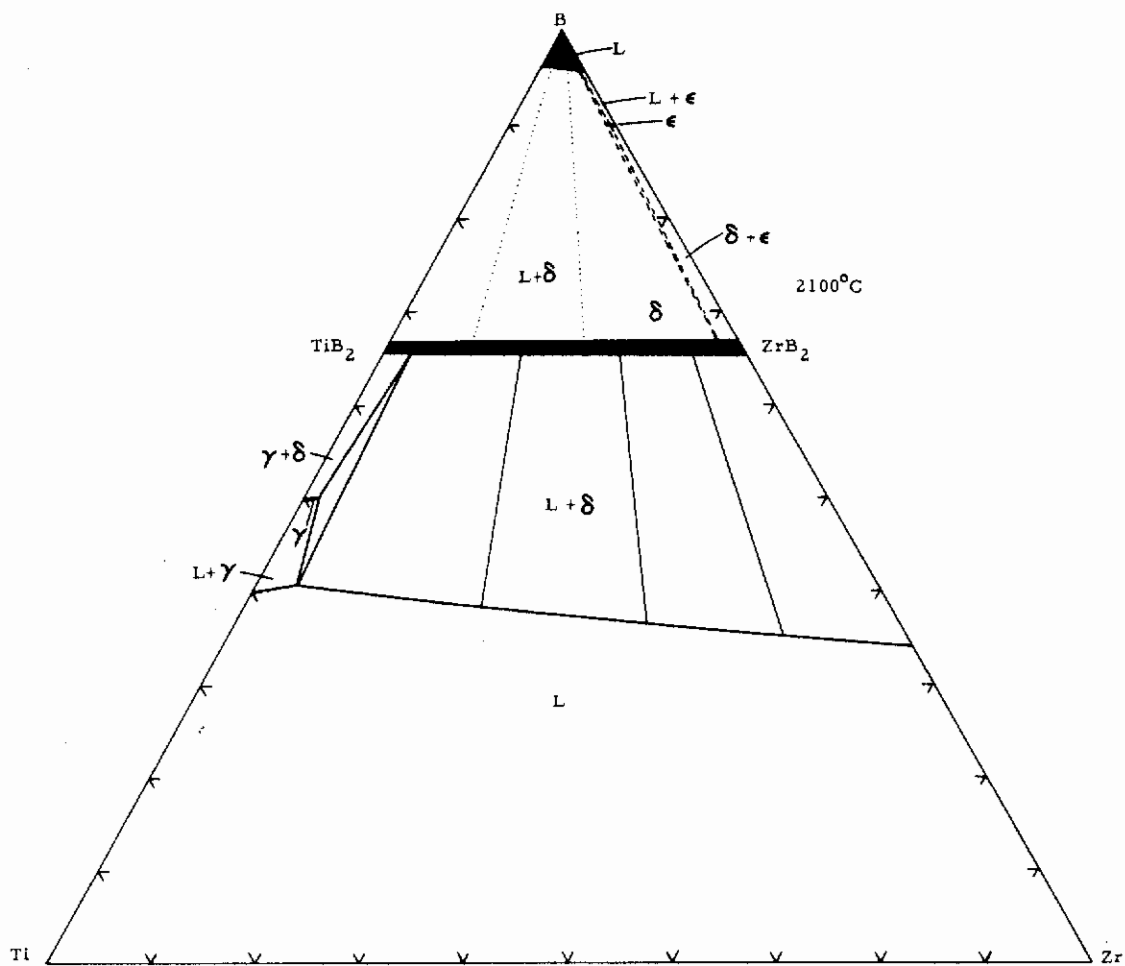


Figure 38. Isothermal Section at 2100°C.

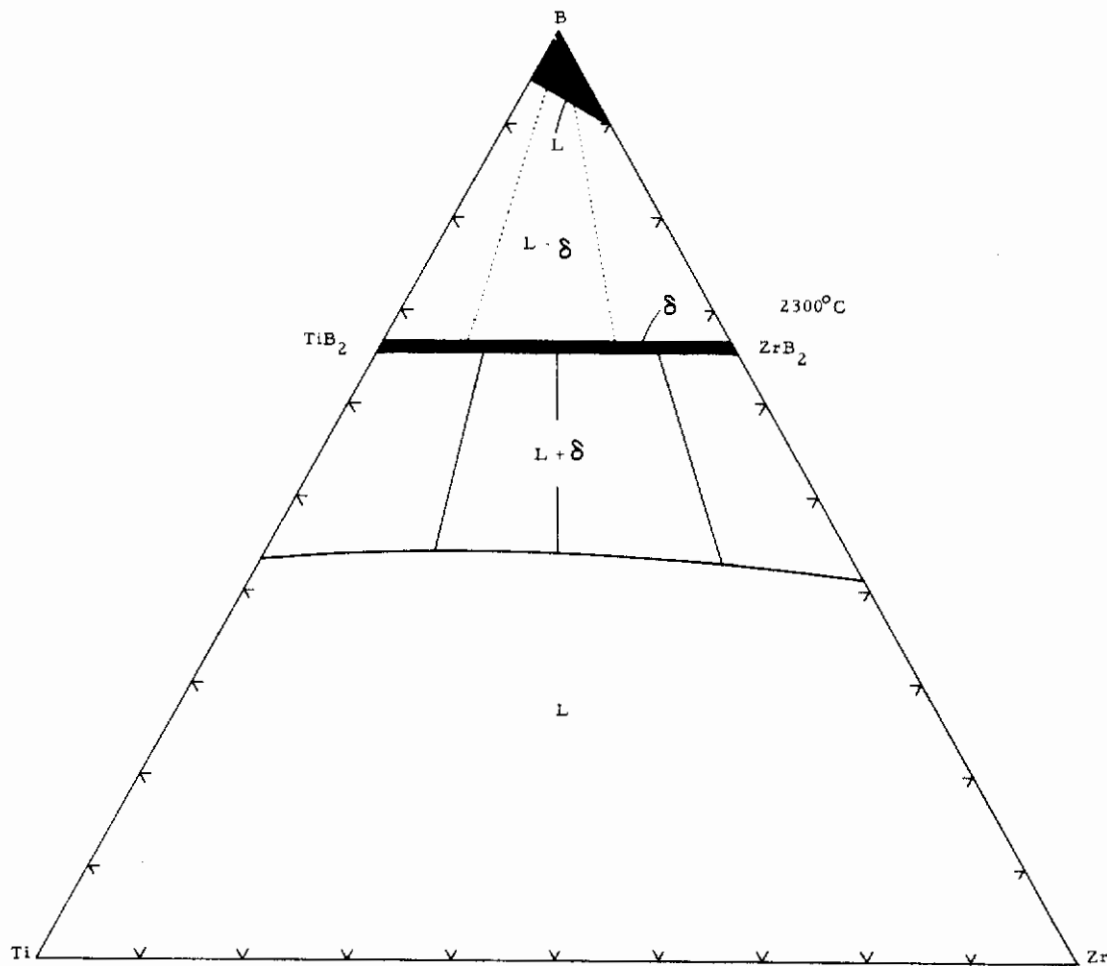


Figure 39. Isothermal Section at 2300°C.

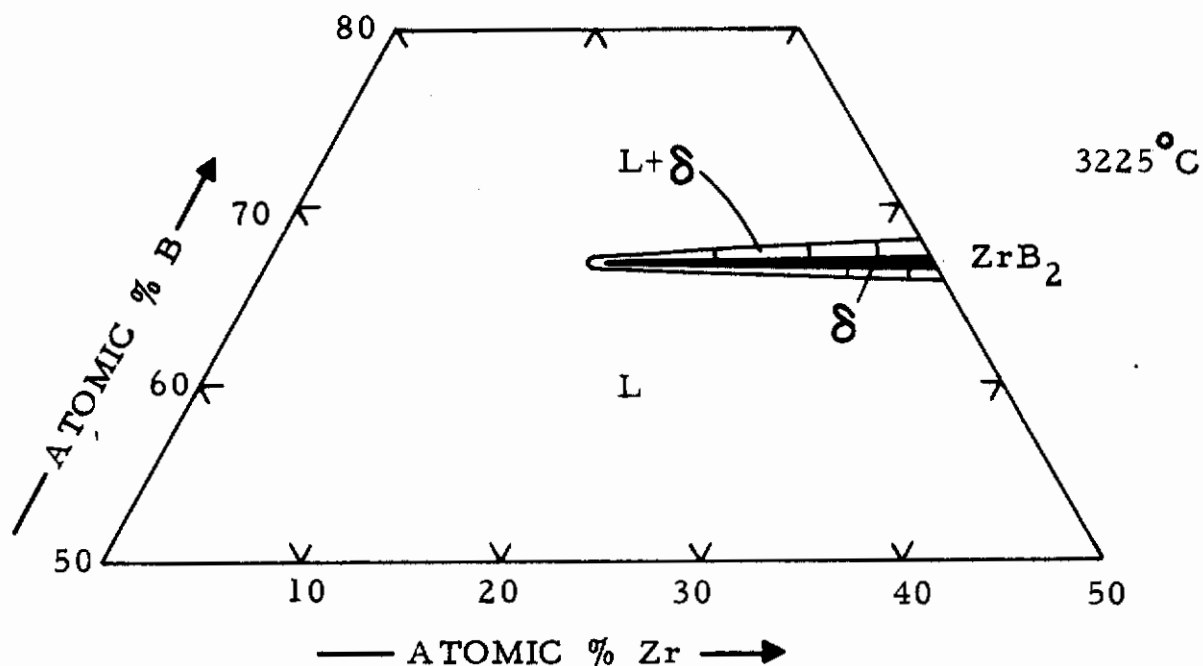


Figure 40. Isothermal Section at 3225°C.

C. INVESTIGATION OF THE MELTING TEMPERATURES OF THE SOLID SOLUTIONS $(\text{Zr}, \text{Nb})\text{B}_2$, $(\text{Zr}, \text{Ta})\text{B}_2$, and $(\text{Hf}, \text{Nb})\text{B}_2$.

Three pseudo-binaries ZrB_2 - NbB_2 , ZrB_2 - TaB_2 , and HfB_2 - NbB_2 were investigated. Plots of the lattice parameters (Figures 41, 43, and 45) confirm the formation of solid solutions in each of the pseudo-binaries studied. The melting point curve of each of the diboride pseudo-binaries varied smoothly between the respective diborides showing no minimum or maximum along the solid solution (Figures 42, 44 and 46).

After melting some samples showed appreciable quantities of unreacted starting materials still present in their Debye-Scherrer powder films. The lattice parameters of such samples were deleted from the lattice parameter plots. Other samples (only in the HfB_2 - NbB_2 pseudo-binary) showed lesser, but not negligible, quantities of unreacted starting materials. These samples have been plotted in Figure 45 with a triangle at the datum point.

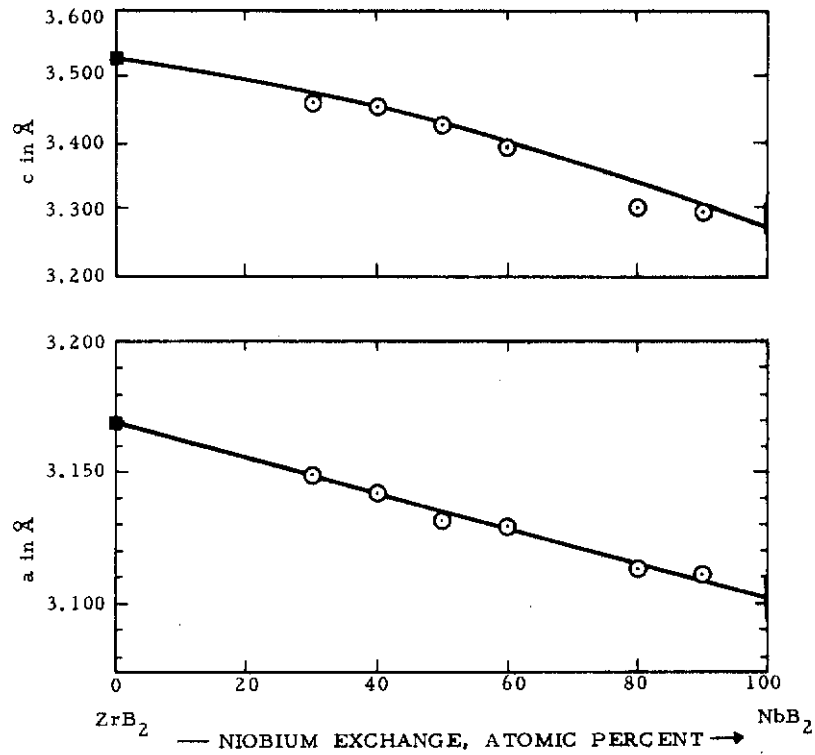


Figure 41. Lattice Parameters of Pseudo-Binary ZrB_2-NbB_2 .

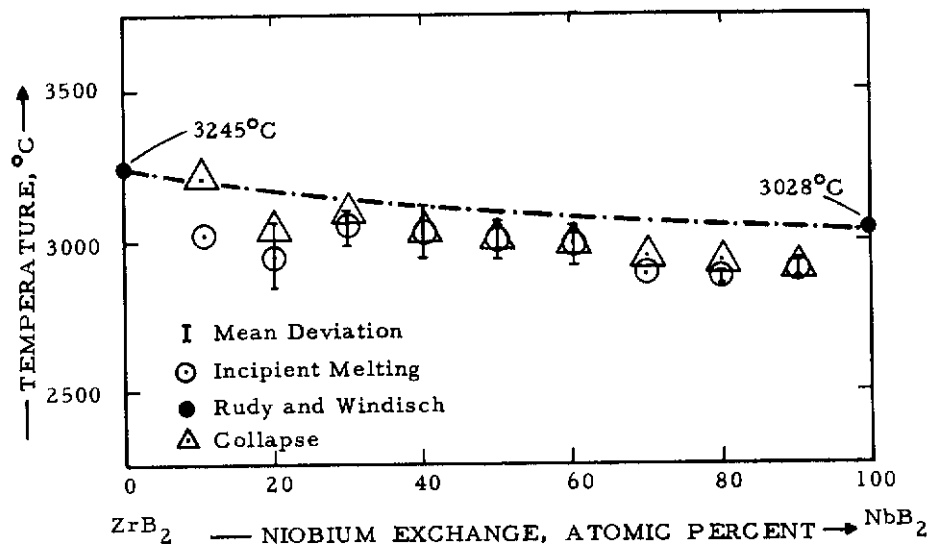


Figure 42. Melting Point Temperatures of Pseudo-Binary ZrB_2-NbB_2 .

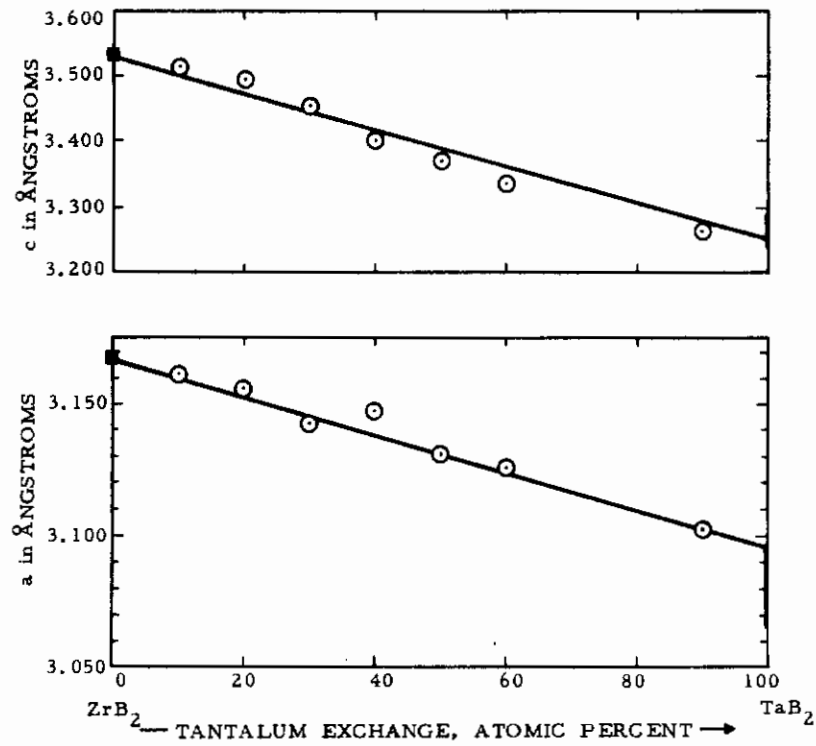


Figure 43. Lattice Parameters of Pseudo-Binary ZrB_2 - TaB_2 .

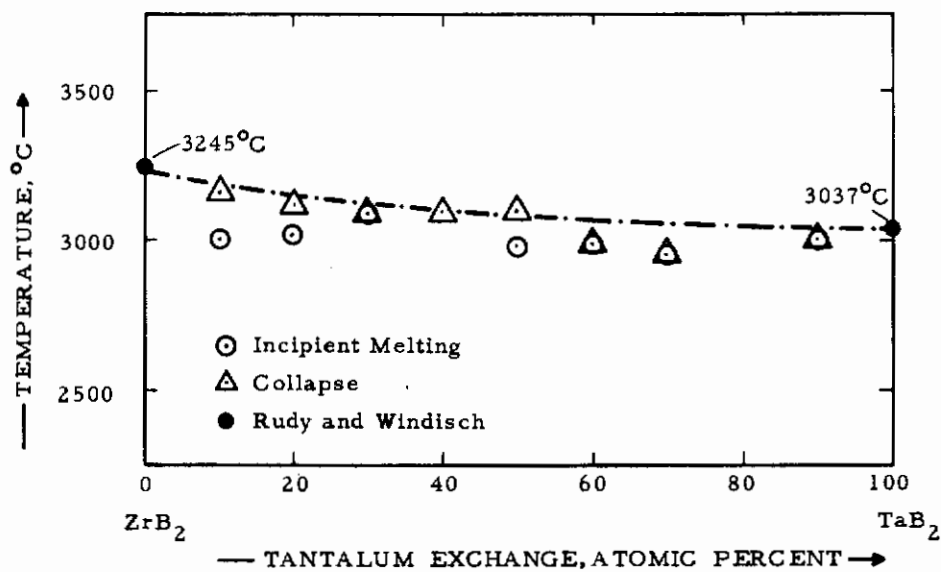


Figure 44. Melting Point Temperatures of Pseudo-Binary ZrB_2 - TaB_2 .

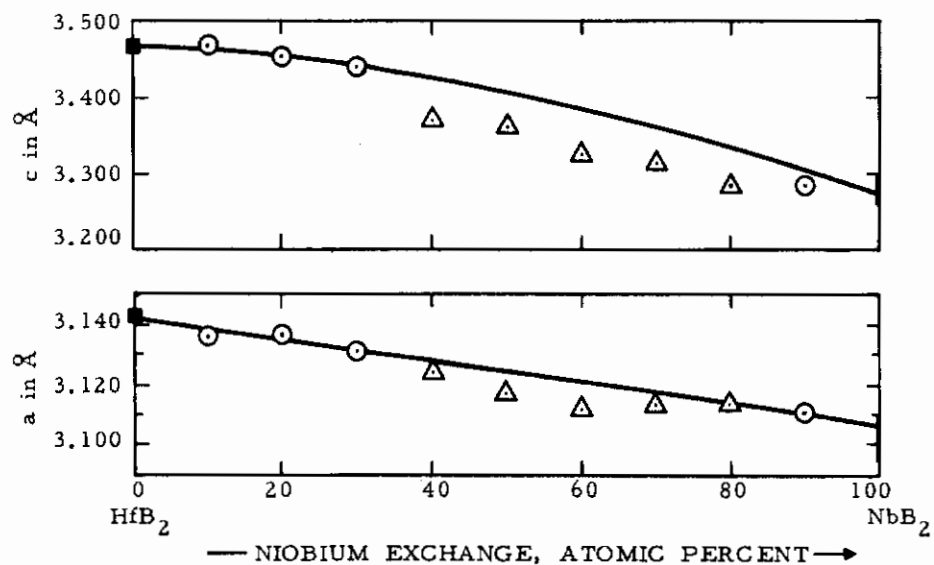


Figure 45. Lattice Parameters of Pseudo-Binary HfB_2 - NbB_2 .

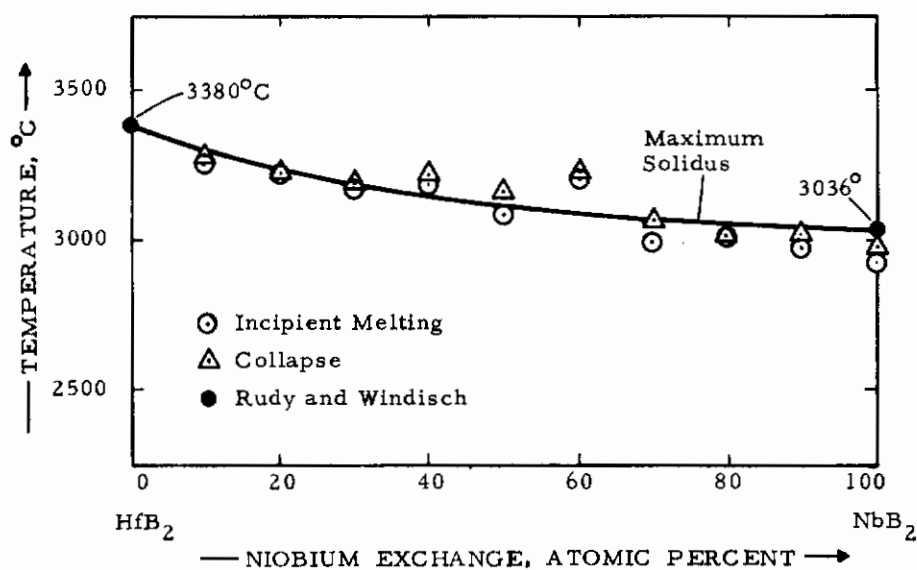


Figure 46. Melting Point Temperatures of Pseudo-Binary HfB_2 - NbB_2 .

The end points in the lattice parameter plots (lattice parameters of the binary diborides) were taken from previous investigations^(4, 5, 15) by Rudy and Windisch. It should be noted that the lattice parameters of TaB_2 and NbB_2 show an appreciable variation; this is due to their wide range of homogeneity in their binary systems. Micrographs of representative samples are shown in Figures 47, 48, and 49.

The lattice parameters and melting points of $(Zr, Nb)B_2$ require no comments except that the melting points are lower than the suggested maximum solidus; the reasons for this are the same as those for the $(TiZr)B_2$ diborides (see page 28). Slight positive deviation from Vegard's law may be noted in the 'c' values, but the 'a' values essentially vary linearly with composition.

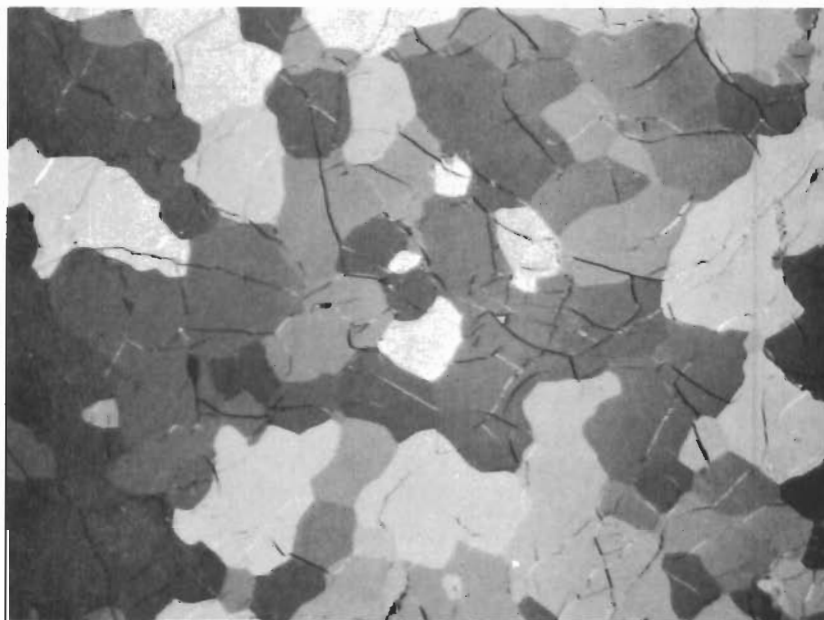


Figure 47. Metallography of ZrB_2 - NbB_2 : 60-40 Mole %.

Cracked $(Zr, Nb)B_2$ Grains with Minute Traces of the Metal Phase at Grain Boundaries. (Polarized Light).

In the pseudo-binary $\text{ZrB}_2\text{-TaB}_2$, one can see the expected temperature lowering of the observed incipient melting from that of the suggested maximum solidus on the ZrB_2 side of the melting point plot (Figure 44). This, of course, is due to the extremely narrow range of homogeneity of ZrB_2 as mentioned several times before. The lattice parameters in this pseudo-binary system essentially follow Vegard's law.

The pseudo-binary $\text{HfB}_2\text{-NbB}_2$ requires no further comment than the previously noted fact that some unreacted starting material remained in some samples (whose data points are triangles in Figure 45).



Figure 48. Metallography of $\text{ZrB}_2\text{-TaB}_2$: 10-90 Mole %.

Cracked $(\text{Zr, Ta})\text{B}_2$ Grains with Minute Traces of Another Boride Phase at Grain Boundaries. (Polarized Light).

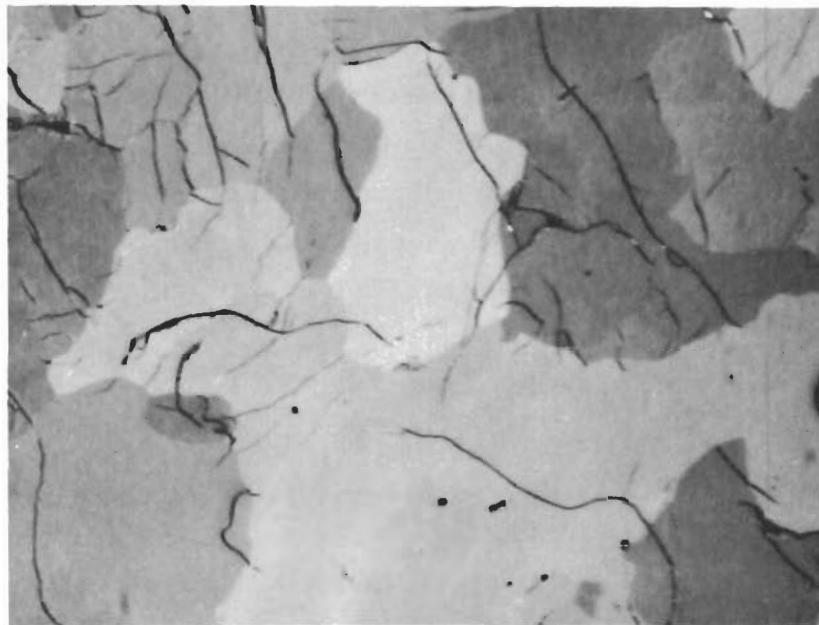


Figure 49. Metallography of $\text{HfB}_2\text{-NbB}_2$; 20-80 Mole % .
Cracked $(\text{Hf}, \text{Nb})\text{B}_2$ Grains. (Polarized Light).

V. DISCUSSION

It is of interest to compare this system to the other group IV transition metal boron systems, Zr-Hf-B⁽¹²⁾ and Ti-Hf-B⁽¹³⁾. The Ti-Zr-B system more closely resembles the Zr-Hf-B system differing from it mostly in that the α - β metal transition in the Ti-Zr-B system occurs at much lower temperatures, and that a minimum in the melting occurs in the Ti-Zr-B ternary. The system Ti-Hf-B differs from the Ti-Zr-B system in that TiB and HfB form a continuous series of solid solutions and thus the diborides in this system are not in equilibrium with metal; whereas, in the system Ti-Zr-B, since ZrB is not stable, a portion of the ternary diboride solid solution is in equilibrium with metal.

Results of this investigation show zirconium diboride to be more stable than titanium diboride (since the tie lines in the two-phase areas point to the zirconium-rich side of the diboride solid solution). This is in agreement with results in the literature⁽¹⁴⁾ determined by other thermo-chemical means.

REFERENCES

1. F.N. Rhines: Phase Diagrams in Metallurgy (McGraw-Hill, 1956).
2. E.T. Hayes, A.H. Roberson, and O.G. Paasche: Bureau of Mines Report of Investigations 4826 (1951).
3. M. Hansen and K. Anderko: Constitution of Binary Alloys, 2nd Edition, (McGraw-Hill, 1958).
4. E. Rudy and St. Windisch: AFML-TR-65-2, Part I, Vol. VII (Jan 1966).
5. E. Rudy and St. Windisch: AFML-TR-65-2, Part I, Vol VIII (Jan 1966).
6. J.T. Norton, H. Blumenthal, and S.J. Sindeband: Met. Trans. 185 (1949), 749.
7. H. Nowotny: Planseeber Pulvermet. Bd 1, (1953), 43.
8. B. Post, F.W. Glaser, and D. Moskowitz: Acta. Met. 2, (1954), 20.
9. F.W. Glaser and W. Ivanick: Powder Met. Bull. 6, No. 4 (1953), 126.
10. G.A. Meerson, G.W. Samsonov, and R.B. Kotelnikov: Izvest. Sek. Fiz. Chim. Anal., Izdat. Akad. Nauk SSSR 25 (1954), 89.
11. E. Rudy, St. Windisch, and Y.A. Chang: AFML-TR-65-2, Part I, Vol. I (1965).
12. D.P. Harmon: AFML-TR-65-2, Part II, Vol. VI (Nov 1965).
13. Y.A. Chang: AFML-TR-65-2, Part II, Vol. V (Nov 1965).
14. L. Kaufman in "Compounds of Interest in Nuclear Reactor Technology (J.T. Waber and P. Chiotti, editors), Metallurgical Soc. of AIME (1964), 193.
15. E. Rudy and St. Windisch: AFML-TR-65-2 (March 1966).

Contrails

DOCUMENT CONTROL DATA - R&D		
(Security classification of title, body of abstract and indexing annotation must be entered when the overall report is classified)		
1. ORIGINATING ACTIVITY (Corporate author) Materials Research Laboratory Aerojet-General Corporation Sacramento, California	2a. REPORT SECURITY CLASSIFICATION <div style="text-align: center; font-weight: bold; padding: 2px;">UNCLASSIFIED</div>	
	2b. GROUP <div style="text-align: center; padding: 2px;">N.A.</div>	
3. REPORT TITLE Ternary Phase Equilibrium in Transition Metal-Boron-Carbon-Silicon Systems. Part II. Ternary Systems. Vol. XII. Ti-Zr-B System. Investigation of Pseudo-Binary Systems ZrB_2-NbB_2 , ZrB_2-TaB_2 , and HfB_2-NbB_2 .		
4. DESCRIPTIVE NOTES (Type of report and inclusive dates) <div style="text-align: center; padding: 2px;">Documentary Report</div>		
5. AUTHOR(S) (Last name, first name, initial) <div style="text-align: center; padding: 10px;">Eckert, T. E.</div>		
6. REPORT DATE <div style="text-align: center; padding: 2px;">October 1966</div>	7a. TOTAL NO. OF PAGES <div style="text-align: center; padding: 2px;">47</div>	7b. NO. OF REFS <div style="text-align: center; padding: 2px;">15</div>
8a. CONTRACT OR GRANT NO. <div style="text-align: center; padding: 2px;">AF 33(615)-1249</div>	9a. ORIGINATOR'S REPORT NUMBER(S) <div style="text-align: center; padding: 2px;">AFML-TR-65-2 Part II, Volume XII</div>	
b. PROJECT NO. 7350	9b. OTHER REPORT NO(S) (Any other numbers that may be assigned this report)	
c. Task No. 735001		
d.		
10. AVAILABILITY/LIMITATION NOTICES This document is subject to special export controls and each transmittal to foreign governments or foreign nationals may be made only with prior approval of Metals & Ceramics Div., AF Materials Laboratory, Wright-Patterson Air Force Base, Ohio.		
11. SUPPLEMENTARY NOTES	12. SPONSORING MILITARY ACTIVITY <div style="text-align: center; padding: 2px;">AFML (MAMC) Wright-Patterson AFB, Ohio 45433</div>	
13. ABSTRACT The ternary system titanium-zirconium-boron was investigated from 1000°C to 3245°C, the melting temperature of zirconium diboride. The equilibria which exist have been determined except for the boron-rich equilibria which have been estimated. The following notable features were found: minimum melting occurs in the titanium rich corner of the ternary; a four-phase reaction involving β -metal phase, monoboride, diboride, and liquid occurs at a temperature slightly higher than the minimum melting; zirconium exchanges with titanium in titanium monoboride to about 9 At.% zirconium; and the metal diborides form a continuous series of solid solutions. No ternary compounds were found. The techniques used in the investigation were X-ray analysis, melting point determination, and metallographic examination. Lattice parameter plots of the pseudo-binary systems ZrB_2-NbB_2 , ZrB_2-TaB_2 , and HfB_2-NbB_2 indicate that in each of these systems the diborides form a continuous series of solid solutions. Melting point temperatures for these systems have been determined. <div style="font-style: italic; padding-top: 10px;">This document has been approved for public release and sale; its distribution is unlimited. U.S.A.F. Systems Command Letter dated Aug. 22, 1968 MAMC (Capt. Marshanda)</div>		

UNCLASSIFIED
Security Classification

14	KEY WORDS	LINK A		LINK B		LINK C	
		ROLE	WT	ROLE	WT	ROLE	WT
<p>Boride High Temperature Phase Equilibria Ternary Systems</p>							

INSTRUCTIONS

1. ORIGINATING ACTIVITY: Enter the name and address of the contractor, subcontractor, grantee, Department of Defense activity or other organization (*corporate author*) issuing the report.

2a. REPORT SECURITY CLASSIFICATION: Enter the overall security classification of the report. Indicate whether "Restricted Data" is included. Marking is to be in accordance with appropriate security regulations.

2b. GROUP: Automatic downgrading is specified in DoD Directive 5200.10 and Armed Forces Industrial Manual. Enter the group number. Also, when applicable, show that optional markings have been used for Group 3 and Group 4 as authorized.

3. REPORT TITLE: Enter the complete report title in all capital letters. Titles in all cases should be unclassified. If a meaningful title cannot be selected without classification, show title classification in all capitals in parenthesis immediately following the title.

4. DESCRIPTIVE NOTES: If appropriate, enter the type of report, e.g., interim, progress, summary, annual, or final. Give the inclusive dates when a specific reporting period is covered.

5. AUTHOR(S): Enter the name(s) of author(s) as shown on or in the report. Enter (last name, first name, middle initial. If military, show rank and branch of service. The name of the principal author is an absolute minimum requirement.

6. REPORT DATE: Enter the date of the report as day, month, year; or month, year. If more than one date appears on the report, use date of publication.

7a. TOTAL NUMBER OF PAGES: The total page count should follow normal pagination procedures, i.e., enter the number of pages containing information.

7b. NUMBER OF REFERENCES: Enter the total number of references cited in the report.

8a. CONTRACT OR GRANT NUMBER: If appropriate, enter the applicable number of the contract or grant under which the report was written.

8b, 8c, & 8d. PROJECT NUMBER: Enter the appropriate military department identification, such as project number, subproject number, system numbers, task number, etc.

9a. ORIGINATOR'S REPORT NUMBER(S): Enter the official report number by which the document will be identified and controlled by the originating activity. This number must be unique to this report.

9b. OTHER REPORT NUMBER(S): If the report has been assigned any other report numbers (*either by the originator or by the sponsor*), also enter this number(s).

10. AVAILABILITY/LIMITATION NOTICES: Enter any limitations on further dissemination of the report, other than those

imposed by security classification, using standard statements such as:

- (1) "Qualified requesters may obtain copies of this report from DDC."
- (2) "Foreign announcement and dissemination of this report by DDC is not authorized."
- (3) "U. S. Government agencies may obtain copies of this report directly from DDC. Other qualified DDC users shall request through _____."
- (4) "U. S. military agencies may obtain copies of this report directly from DDC. Other qualified users shall request through _____."
- (5) "All distribution of this report is controlled. Qualified DDC users shall request through _____."

If the report has been furnished to the Office of Technical Services, Department of Commerce, for sale to the public, indicate this fact and enter the price, if known.

11. SUPPLEMENTARY NOTES: Use for additional explanatory notes.

12. SPONSORING MILITARY ACTIVITY: Enter the name of the departmental project office or laboratory sponsoring (*paying for*) the research and development. Include address.

13. ABSTRACT: Enter an abstract giving a brief and factual summary of the document indicative of the report, even though it may also appear elsewhere in the body of the technical report. If additional space is required, a continuation sheet shall be attached.

It is highly desirable that the abstract of classified reports be unclassified. Each paragraph of the abstract shall end with an indication of the military security classification of the information in the paragraph, represented as (TS), (S), (C), or (U).

There is no limitation on the length of the abstract. However, the suggested length is from 150 to 225 words.

14. KEY WORDS: Key words are technically meaningful terms or short phrases that characterize a report and may be used as index entries for cataloging the report. Key words must be selected so that no security classification is required. Identifiers, such as equipment model designation, trade name, military project code name, geographic location, may be used as key words but will be followed by an indication of technical context. The assignment of links, rules, and weights is optional.

UNCLASSIFIED